STANFORD UNIVERSITY

Modeling aspects of forming and switching in RRAM devices, including possible doping effects for improved characteristics

Blanka Magyari-Köpe and Yoshio Nishi
Stanford University

Current Students: Liang Zhao, Dan Duncan

Former Students: Dr. Seong-Geon Park (Samsung), Dr. Hyung-Dong Lee (Hynix)

Collaborators: Prof. Kenji Shiraishi, Prof. Katsumasa Kamiya, MoonYoung Yang (Tsukuba & Nagoya University, Kanagawa Institute of Technology)

RRAM as Emerging Memory

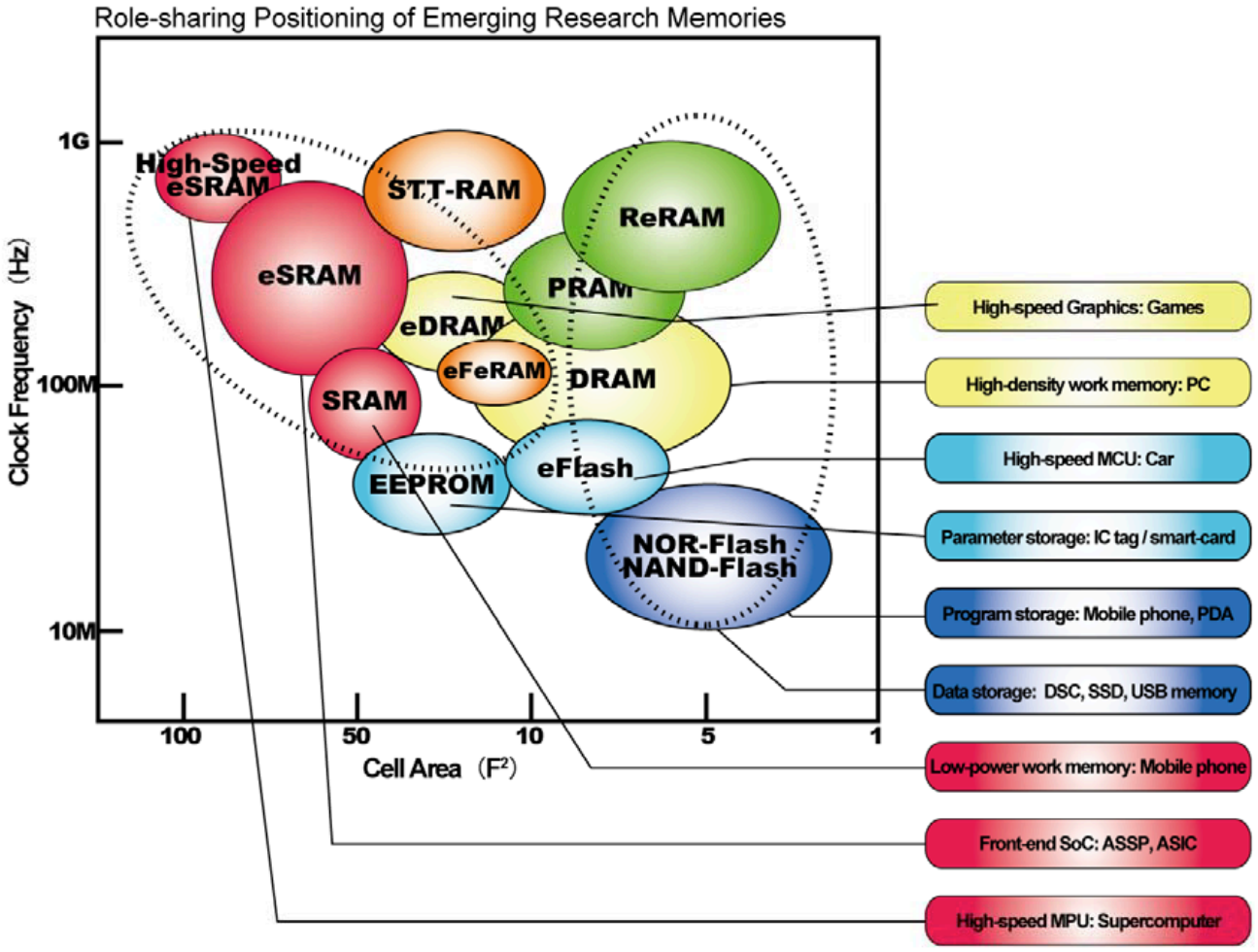

Web of Science Citations for RRAM and ReRAM

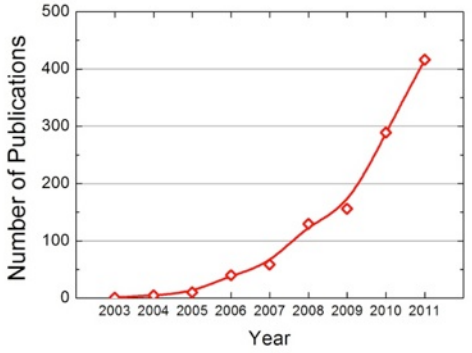

H. Akinaga, AIST, Maturity Evaluation for Selected Emerging Research Memory Technologies, 2010.

Metal Oxide M-I-M Memory (RRAM)

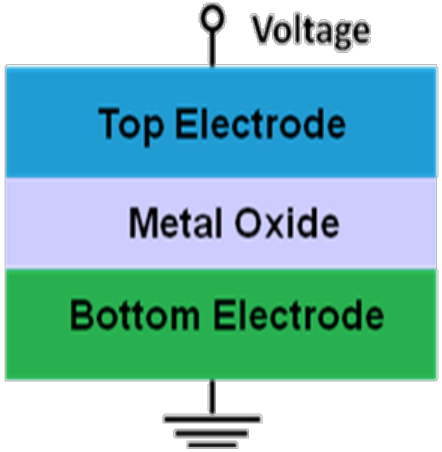

- **Advantages:**
  - Low programming voltage (< 3V)
  - Material set compatible with conventional semiconductor processing (e.g Ni, Hf, Al, Ti, Ta,…)
  - Low temperature processing (BEOL-compatible)
  - High speed and density
  - Structural simplicity
- **Key issues to be resolved:**
  - **Physics of the resistive switching**
  - Device scaling properties
  - Device uniformity
  - Endurance and retention

RRAM Materials Choices

The Periodic Table of the Elements

corresponding binary oxide that exhibits bistable resistance switching

metal that is used for electrode

1 H Hydrogen 1.00794																	2 He Helium 4.003
3 Li Lithium 6.941	4 Be Beryllium 9.012182											5 B Boron 10.811	6 C Carbon 12.0107	7 N Nitrogen 14.00674	8 O Oxygen 15.9994	9 F Fluorine 18.9984032	10 Ne Neon 20.1797
11 Na Sodium 22.989770	12 Mg Magnesium 24.3050											13 Al Aluminum 26.981538	14 Si Silicon 28.0855	15 P Phosphorus 30.973761	16 S Sulfur 32.066	17 Cl Chlorine 35.4527	18 Ar Argon 39.948
19 K Potassium 39.0983	20 Ca Calcium 40.078	21 Sc Scandium 44.955910	22 Ti Titanium 47.867	23 V Vanadium 50.9415	24 Cr Chromium 51.9961	25 Mn Manganese 54.938049	26 Fe Iron 55.845	27 Co Cobalt 58.933200	28 Ni Nickel 58.6934	29 Cu Copper 63.546	30 Zn Zinc 65.39	31 Ga Gallium 69.723	32 Ge Germanium 72.61	33 As Arsenic 74.92160	34 Se Selenium 78.96	35 Br Bromine 79.904	36 Kr Krypton 83.80
37 Rb Rubidium 85.4678	38 Sr Strontium 87.62	39 Y Yttrium 88.90585	40 Zr Zirconium 91.224	41 Nb Niobium 92.90638	42 Mo Molybdenum 95.94	43 Tc Technetium (98)	44 Ru Ruthenium 101.07	45 Rh Rhodium 102.90550	46 Pd Palladium 106.42	47 Ag Silver 107.8682	48 Cd Cadmium 112.411	49 In Indium 114.818	50 Sn Tin 118.710	51 Sb Antimony 121.760	52 Te Tellurium 127.60	53 I Iodine 126.90447	54 Xe Xenon 131.29
55 Cs Cesium 132.90545	56 Ba Barium 137.327	57 La Lanthanum 138.9055	72 Hf Hafnium 178.49	73 Ta Tantalum 180.9479	74 W Tungsten 183.84	75 Re Rhenium 186.207	76 Os Osmium 190.23	77 Ir Iridium 192.217	78 Pt Platinum 195.078	79 Au Gold 196.96655	80 Hg Mercury 200.59	81 Tl Thallium 204.3833	82 Pb Lead 207.2	83 Bi Bismuth 208.98038	84 Po Polonium (209)	85 At Astatine (210)	86 Rn Radon (222)
87 Fr Francium (223)	88 Ra Radium (226)	89 Ac Actinium (227)	104 Rf Rutherfordium (261)	105 Db Dubnium (262)	106 Sg Seaborgium (263)	107 Bh Bohrium (262)	108 Hs Hassium (265)	109 Mt Meitnerium (266)	110 (269)	111 (272)	112 (277)	113	114				

58 Ce Cerium 140.116	59 Pr Praseodymium 140.90765	60 Nd Neodymium 144.24	61 Pm Promethium (145)	62 Sm Samarium 150.36	63 Eu Europium 151.964	64 Gd Gadolinium 157.25	65 Tb Terbium 158.92534	66 Dy Dysprosium 162.50	67 Ho Holmium 164.93032	68 Er Erbium 167.26	69 Tm Thulium 168.93421	70 Yb Ytterbium 173.04	71 Lu Lutetium 174.967
90 Th Thorium 232.0381	91 Pa Protactinium 231.03588	92 U Uranium 238.0289	93 Np Neptunium (237)	94 Pu Plutonium (244)	95 Am Americium (243)	96 Cm Curium (247)	97 Bk Berkelium (247)	98 Cf Californium (251)	99 Es Einsteinium (252)	100 Fm Fermium (257)	101 Md Mendelevium (258)	102 No Nobelium (259)	103 Lr Lawrencium (262)

Unipolar and/or Bipolar Switching

Binary oxides/transition metal oxides **Perovskites**

Nb2O5		TiO2	CuMnOx	SrTiO3
MgO	ZnO	NiO	CuxO	Cr-SrZrO3
Fe2O3	CoO	Ta2O5	CuMoOx	PrCaMnO3
		HfO2	InZnO	SrLaTiO3
		Al2O3		LaSrFeO3

Unipolar

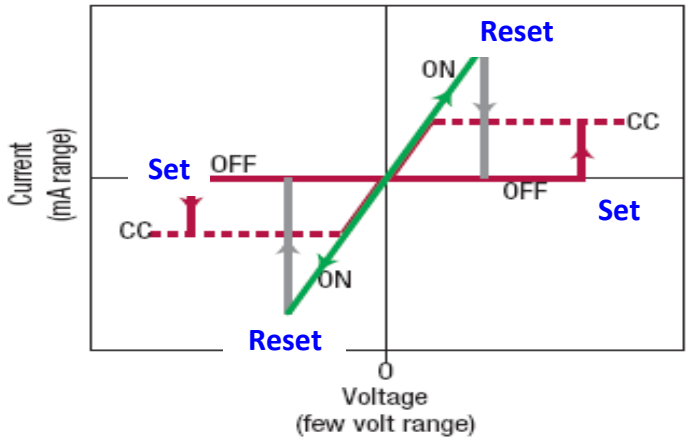

Bipolar

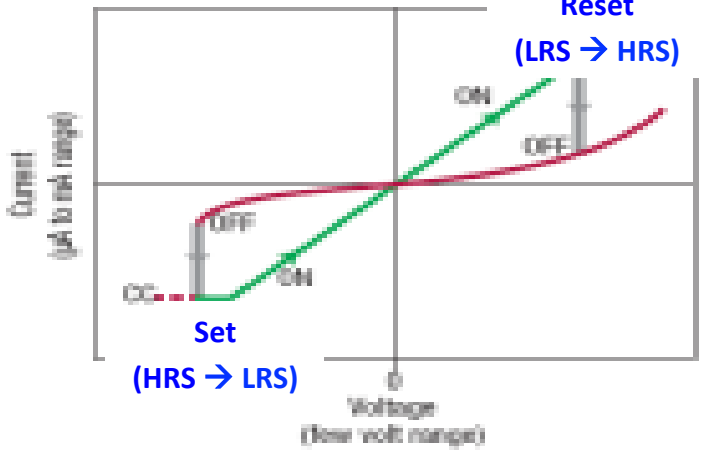

Models for Forming and Resistive Switching

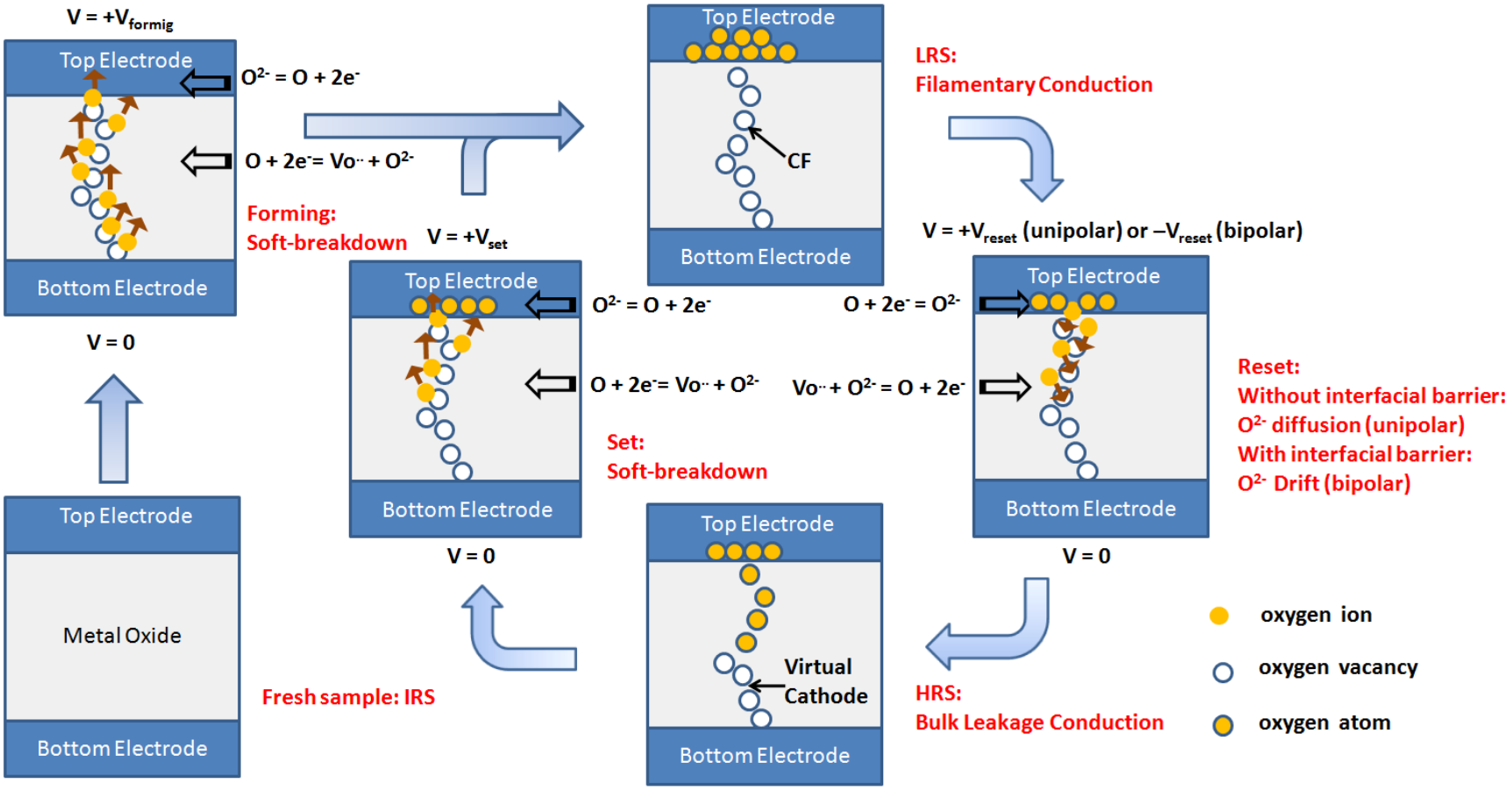

S. Yu, B. Lee, H.-S. P. Wong, "Metal Oxide Memory," in J. Wu, W. Han, H.-C. Kim, A. Janotti eds, "Functional Metal Oxide Nanostructures," Springer 2011.

Theoretical Methods and Analysis

First principles calculations: density functional theory

Electrons: Schrödinger equation: $H\Psi=E\Psi$

$$\hat{H} = \sum_{i=1}^{N} \left(-\sum_{\mathbf{R}} \frac{Ze^2}{|\mathbf{r_i} - \mathbf{R}|} - \frac{\hbar^2 {\nabla_i}^2}{2m} \right) + \frac{1}{2} \sum_{i \neq j} \frac{e^2}{|\mathbf{r_i} - \mathbf{r_j}|}$$

Ions: Geometry optimization

Self-consistent calculation: total energy minimization techniques

Beyond LDA, GGA approximations:
=> on-site Coulomb corrections by introducing Hubbard U in the Hamiltonian

Electronic Structure: VASP

Outline

ON-state Conduction and Filament Formation: TiO_2, NiO, HfO_2, Al_2O_3

The Role of Dopants in Switching: TiO_2, HfO_2

Charge Trapping: TiO_2, HfO_2, Al_2O_3

Thermodynamics: Oxygen Diffusion in/out of the Filament: TiO_2

Electrode/Oxide Interfaces and Electronic Transport

Multilayer structures

Summary

Conductive Filaments of O Vacancies (I)

TiO_2

V_O-chains

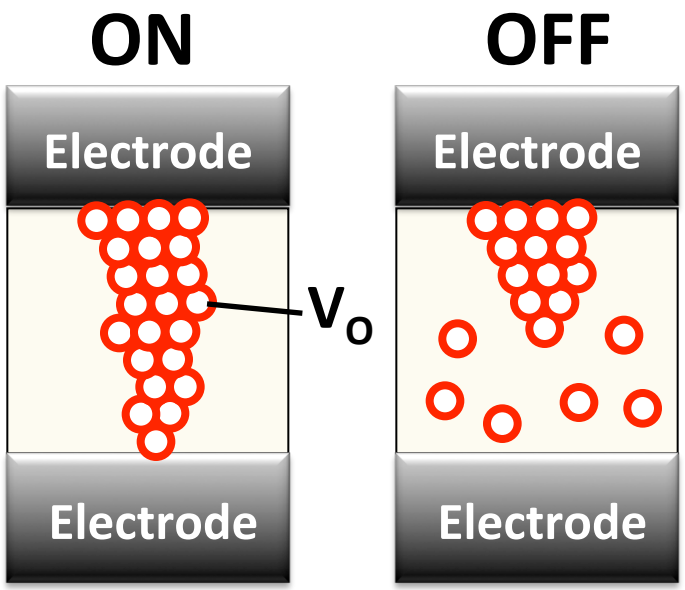

HRTEM images

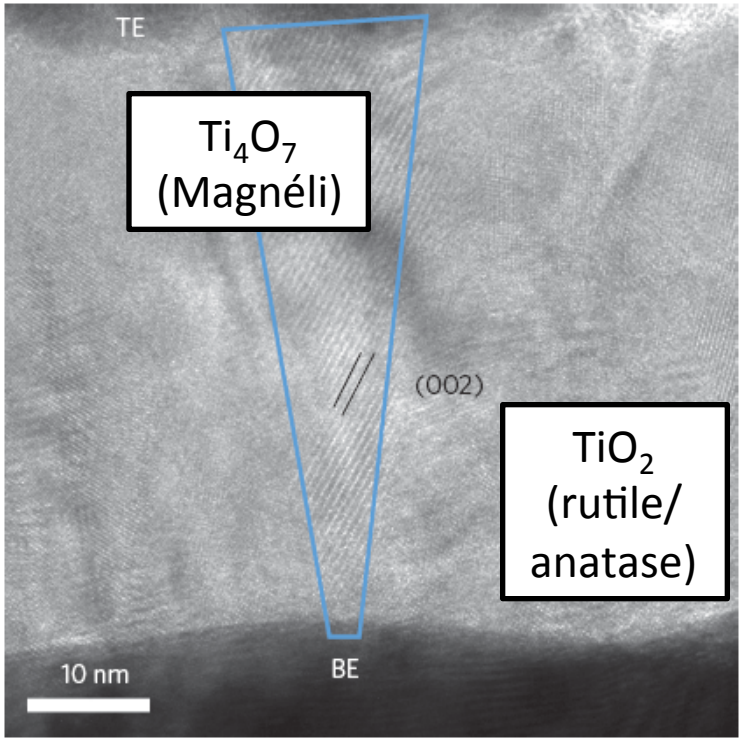

D.-H. Kwon, Nat. Nanotech. 2010

- 5～10 nm diameter Magnéli phase of conical shape observed between the electrodes - electrical conduction path.

Conductive Filaments of O Vacancies (II)

Vacancy ordering in TiO_2

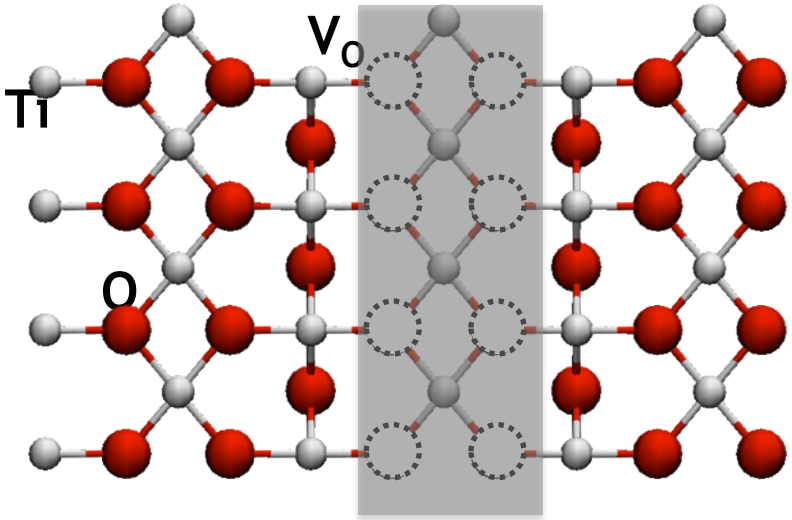

Partial charge density

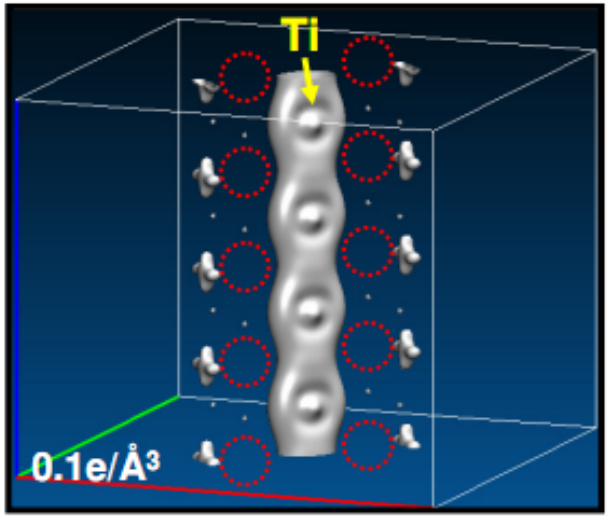

K. Kamiya et al. APL 2012; S.G. Park et al. EDL 2011; Magyari-Kope et al. Nanotechnology 2011; Magyari-Kope et al. J. Mat. Sci. 2012, Zhao et al. APL 2013

- Conductive filaments mediated by V_O chains - "ON" state.

TiO_2: Stability of Multi Vacancy Configurations

$$E_{vf} = E(TiO_{2-x}) - E(TiO_2) + n/2E(O_2)$$

$E(TiO_{2-x})$: The total energy of a supercell containing oxygen vacancies
$E(TiO_2)$: The total energy of a perfect TiO_2 in the same size of supercell
$E(O_2)$: The energy of oxygen molecule
n : The number of oxygen vacancy

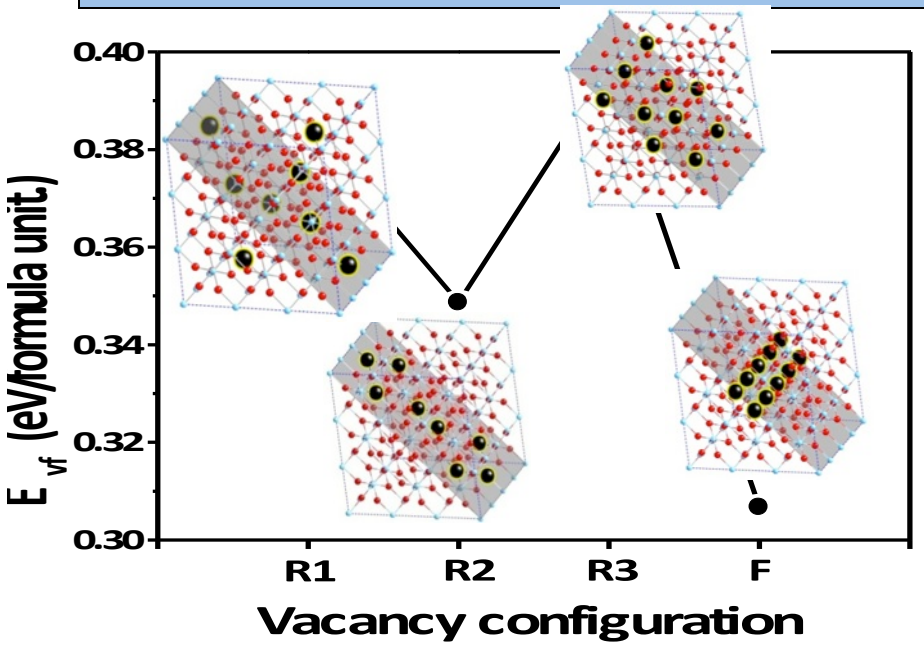

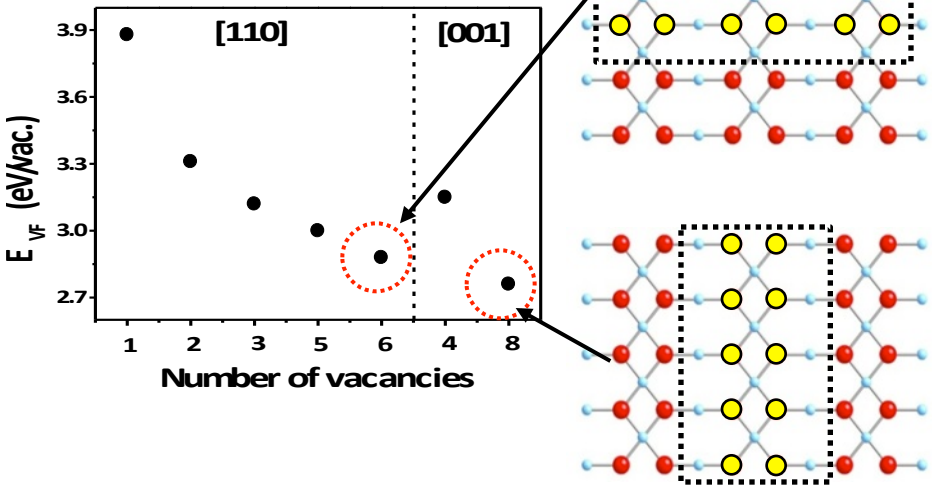

B. Magyari-Köpe, S. G. Park, H.D. Lee, Y. Nishi, J. Mater. Sci., 2012.
B. Magyari-Köpe, M. Tendulkar, S.G. Park, H.D. Lee, Y. Nishi, Nanotechn. 22, 254029, 2011.
S.G. Park, B. Magyari-Köpe, Y. Nishi, EDL 32, 197, 2011.

TiN/HfO_2: Vacancy Filaments

- Monovacancy chain of 8 V_o's

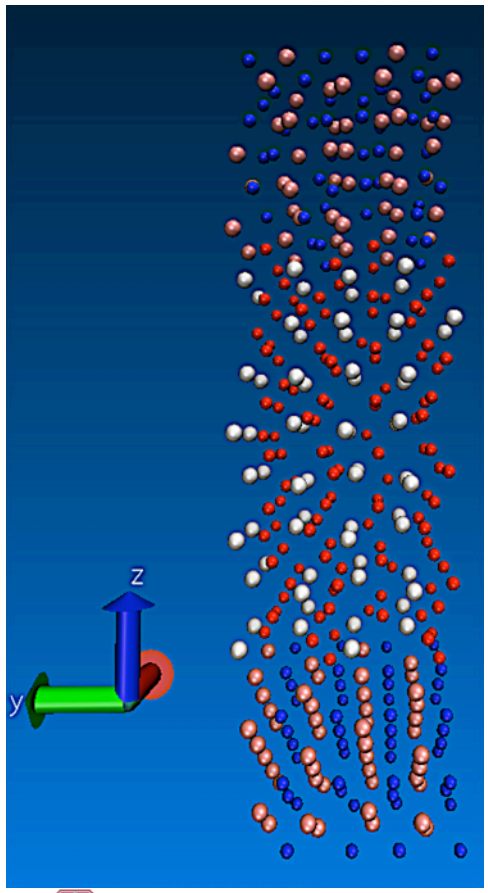

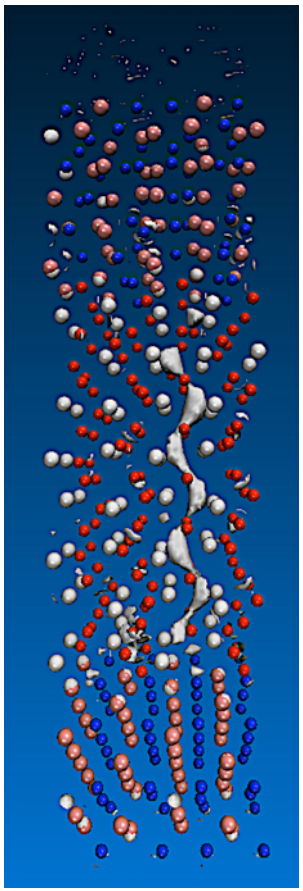

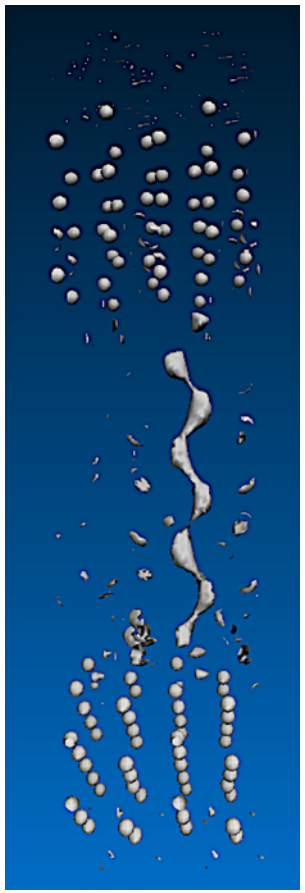

NiO: V_O Filament Configuration

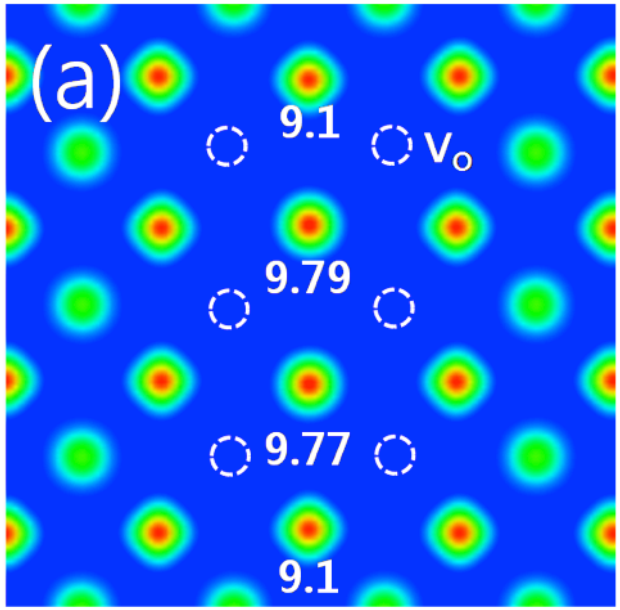

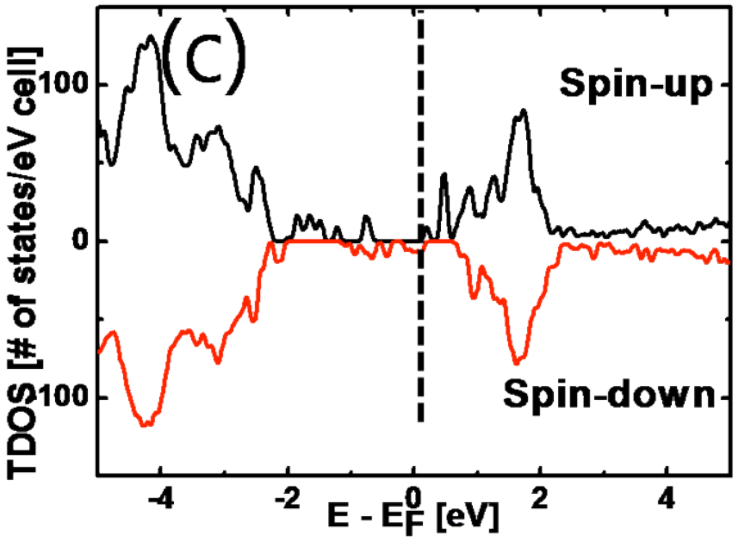

Metallic filament along the <110> direction

2 types of Ni atoms:
- **with 4 V_o (NN)**
- **with 2 V_o (NN)**

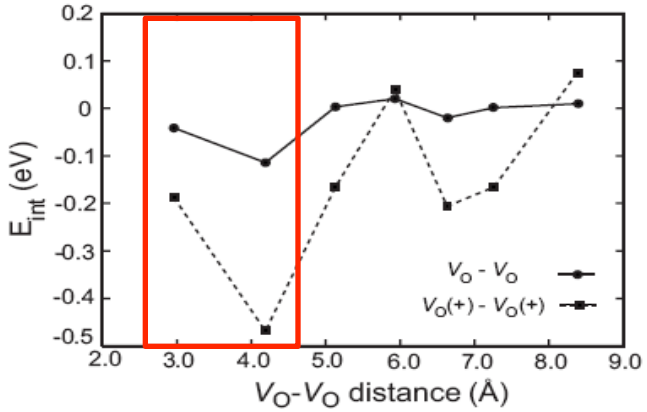

Low V_O-V_O interaction energy

H. Lee, B. Magyari-Köpe, Y. Nishi, PRB 81, 193202,2010

S. Park et al., PRB 77, 134103, 2008.

Conductive Filaments in TiO_2, HfO_2 and Al_2O_3

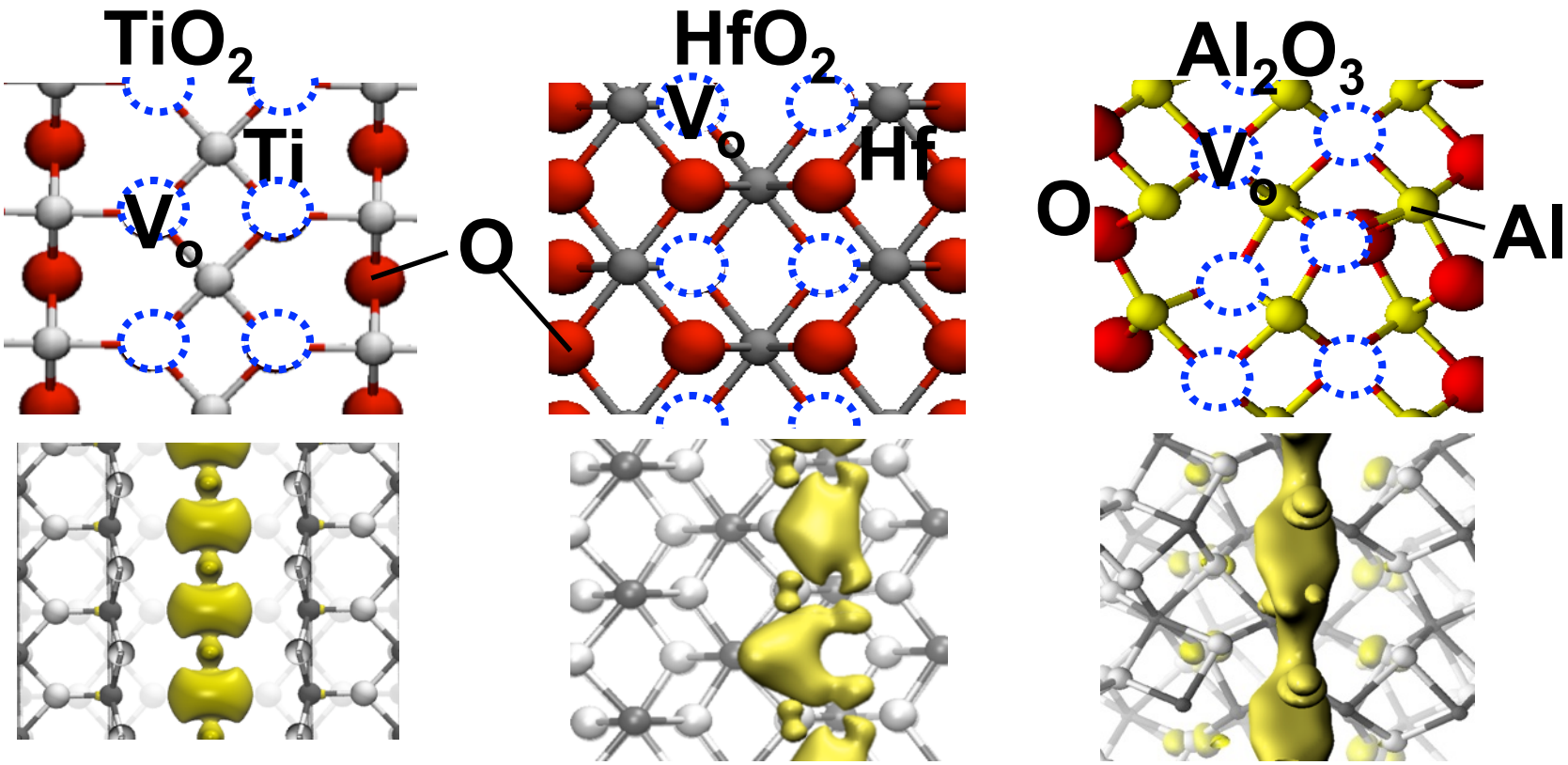

S. Park et al., EDL 2011
K. Kamiya et al., APL 2013

K. Kamiya et al., PRB 2013

M. Yang et al., JJAP 2013

Outline

ON-state Conduction and Filament Formation: TiO_2, NiO, HfO_2, Al_2O_3

The Role of Dopants in Switching: TiO_2, HfO_2

Charge Trapping: TiO_2, HfO_2, Al_2O_3

Thermodynamics: Oxygen Diffusion in/out of the Filament: TiO_2

Electrode/Oxide Interfaces and Electronic Transport

Multilayer structures

Summary

Transition Metal Doping Effects in TiO_2

- Incorporation of Ni, Cu or Sr in a TiO_2 substrate reduces the formation energy of an oxygen vacancy next to the dopant.
- Dopant engineering: lowering the forming voltage and switching energy consumptions.

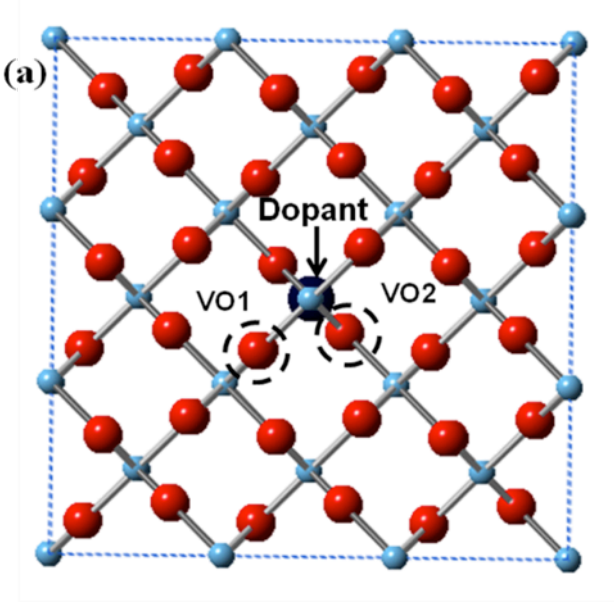

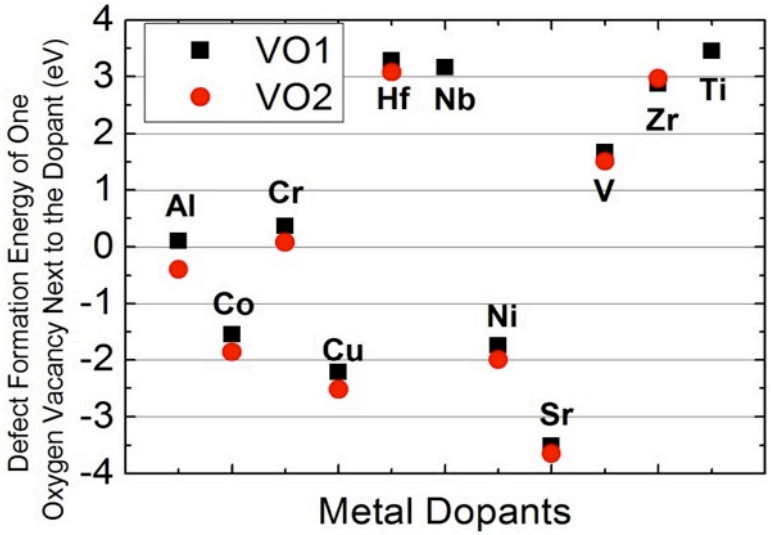

L. Zhao, S.G. Park, B. Magyari-Köpe, and Y. Nishi, SSDM 2012, APL 2013

Choosing the dopants?

- Conductive filament modeled as oxygen vacancy chain
- Systems with different kinds of dopants are studied

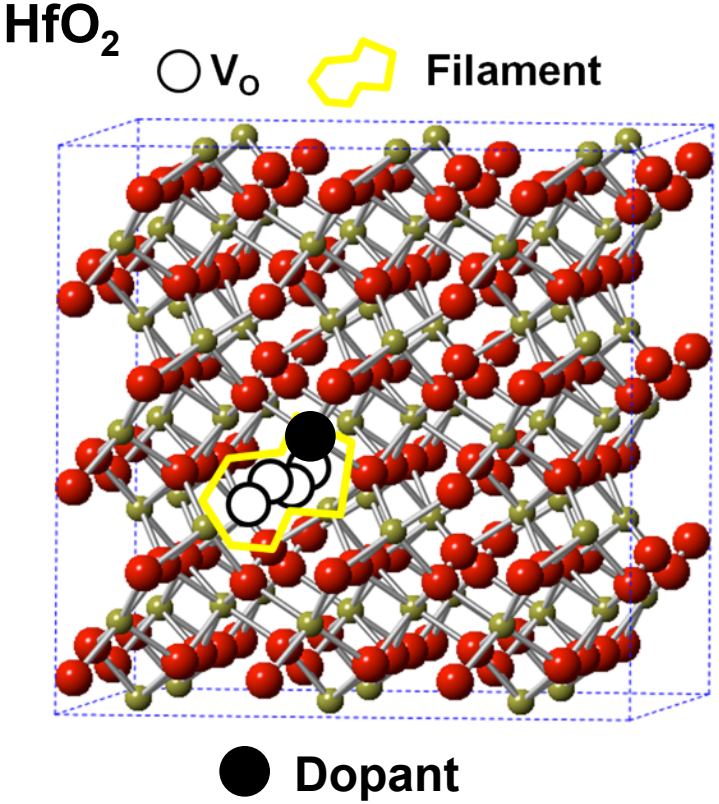

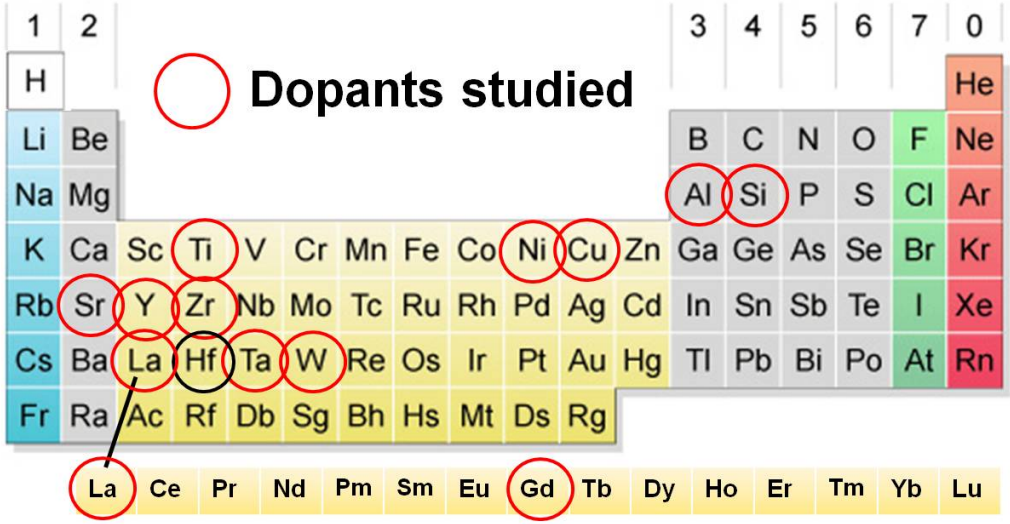

Valence electron number: a key factor in classifying the doping effects

TiO_2: P-type and N-type Transition Metal Doping

$$E_{form} = E_{tot,dopant,V_O} - E_{tot,dopant} + n_{V_O}\mu_O$$

Dopant next to a single V_O

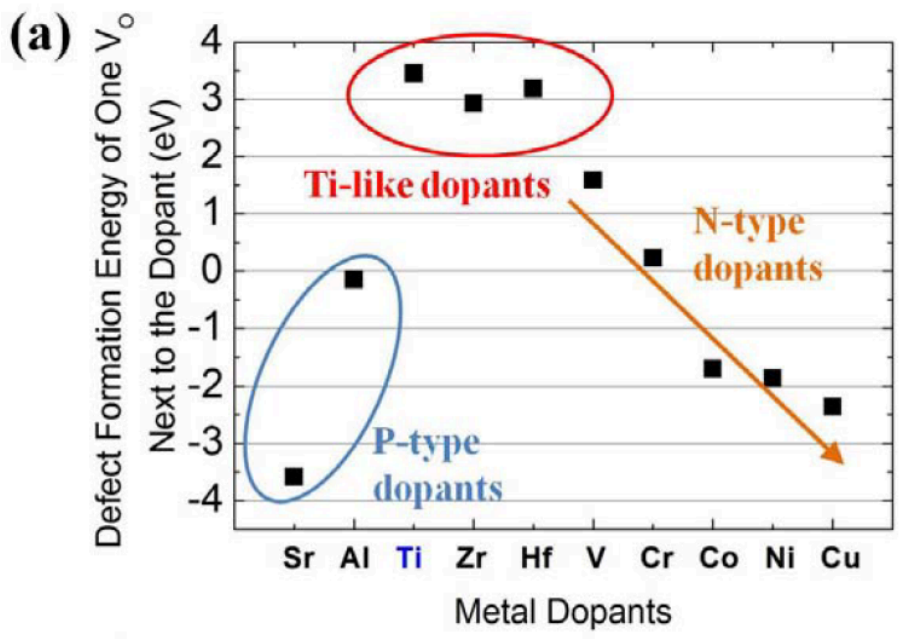

Dopants next to a V_O filament

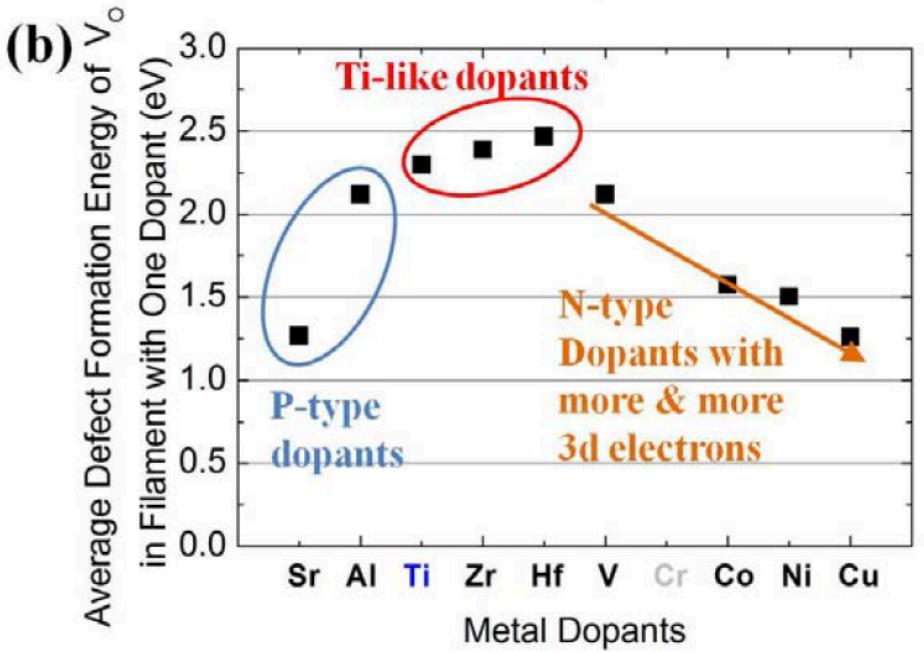

L. Zhao, S.G. Park, B. Magyari-Köpe, and Y. Nishi, APL 2013.

TiO_2: Density of States of Dopants + V_O

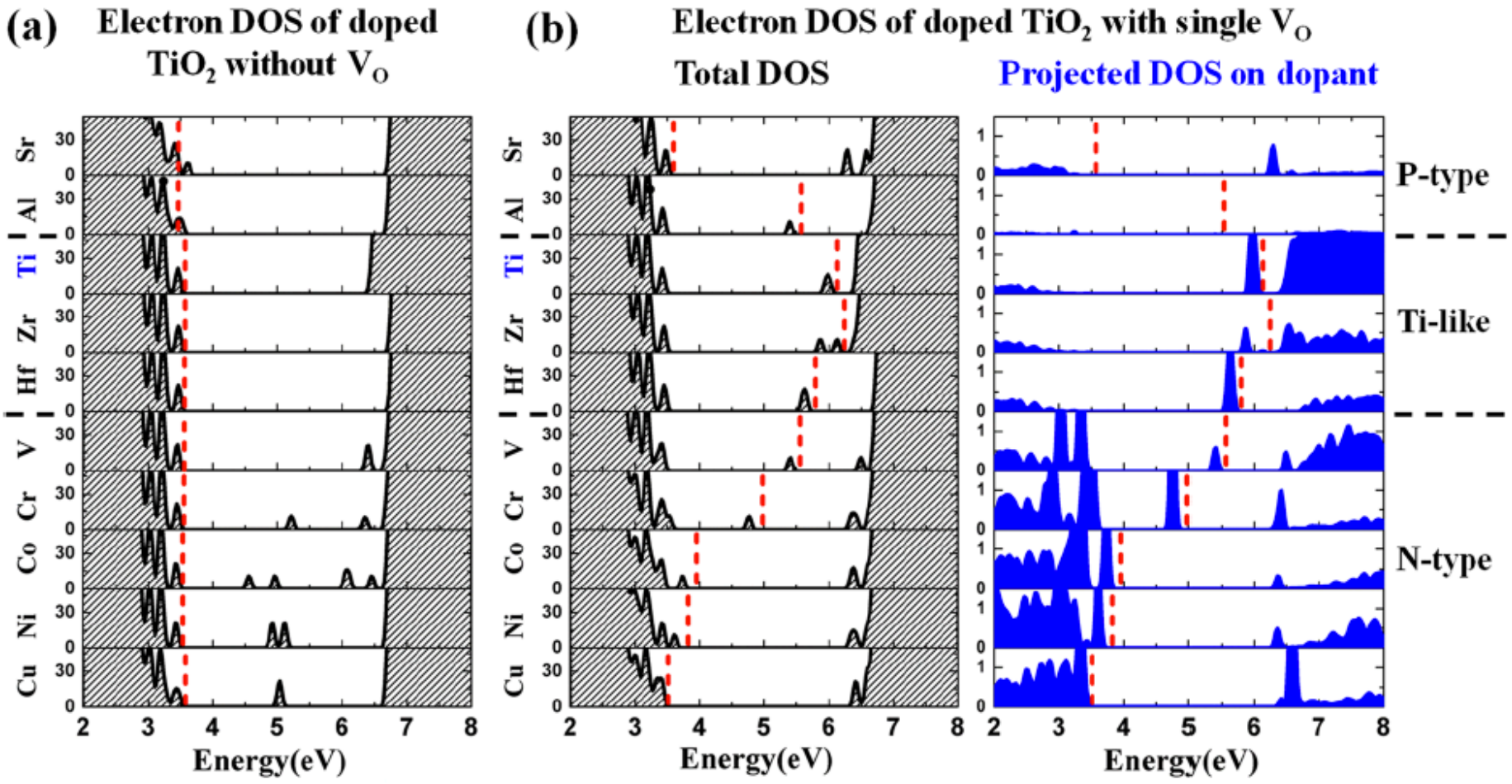

L. Zhao, S.G. Park, B. Magyari-Köpe, and Y. Nishi, APL 2013.

TiO_2: Band Structure Effects of Doping

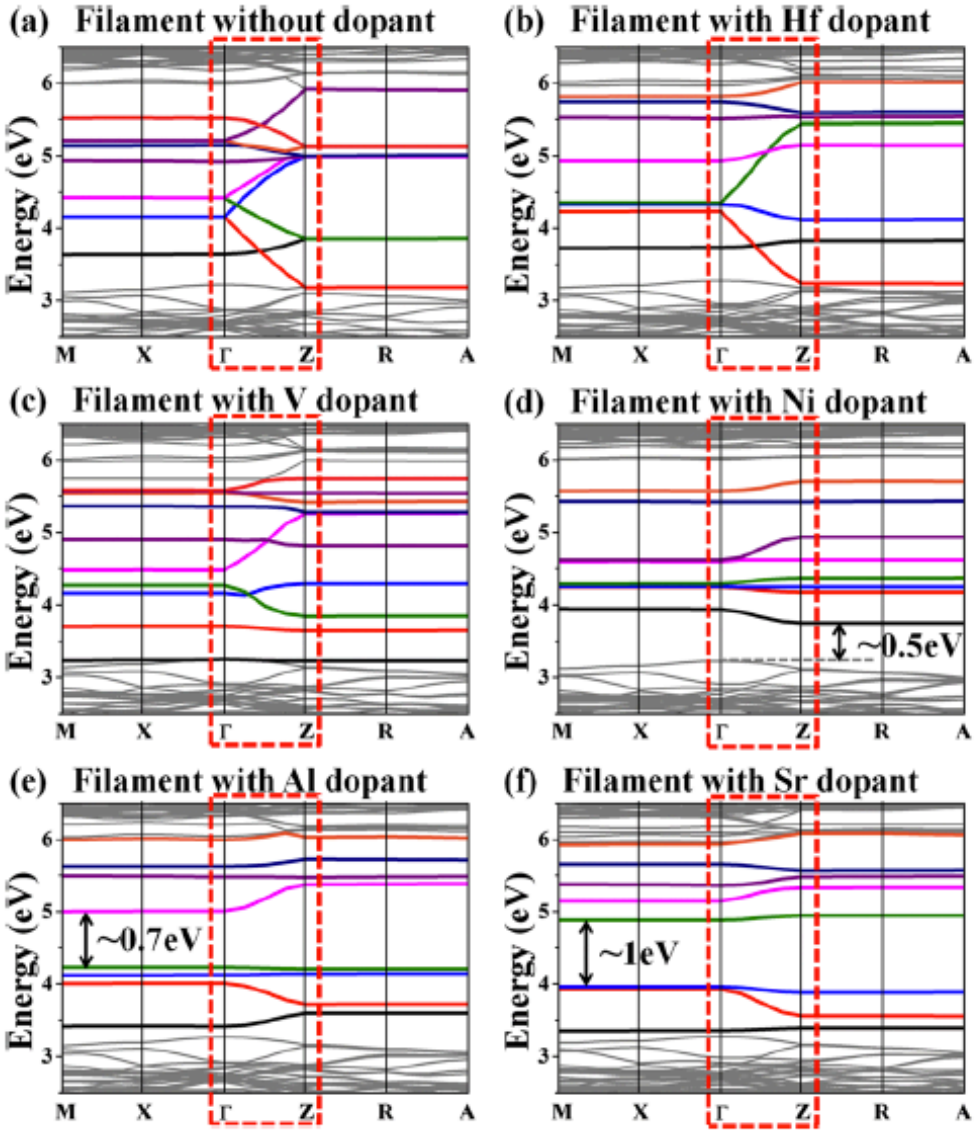

Ti like dopants

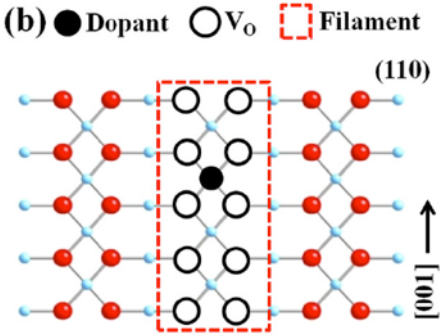

N-type dopants

P-type dopants

L. Zhao, S.G. Park, B. Magyari-Köpe, and Y. Nishi, APL 2013.

HfO_2: Electron Density of States of V_O + Dopant

La doping - D. Liu & J. Robertson, APL 94, 042904, 2009
N doping - K. Xiong, J. Robertson & S. J. Clark, JAP, 99, 044105 2006
F doping - K. Tse & J. Robertson, APL 89, 142914 2006

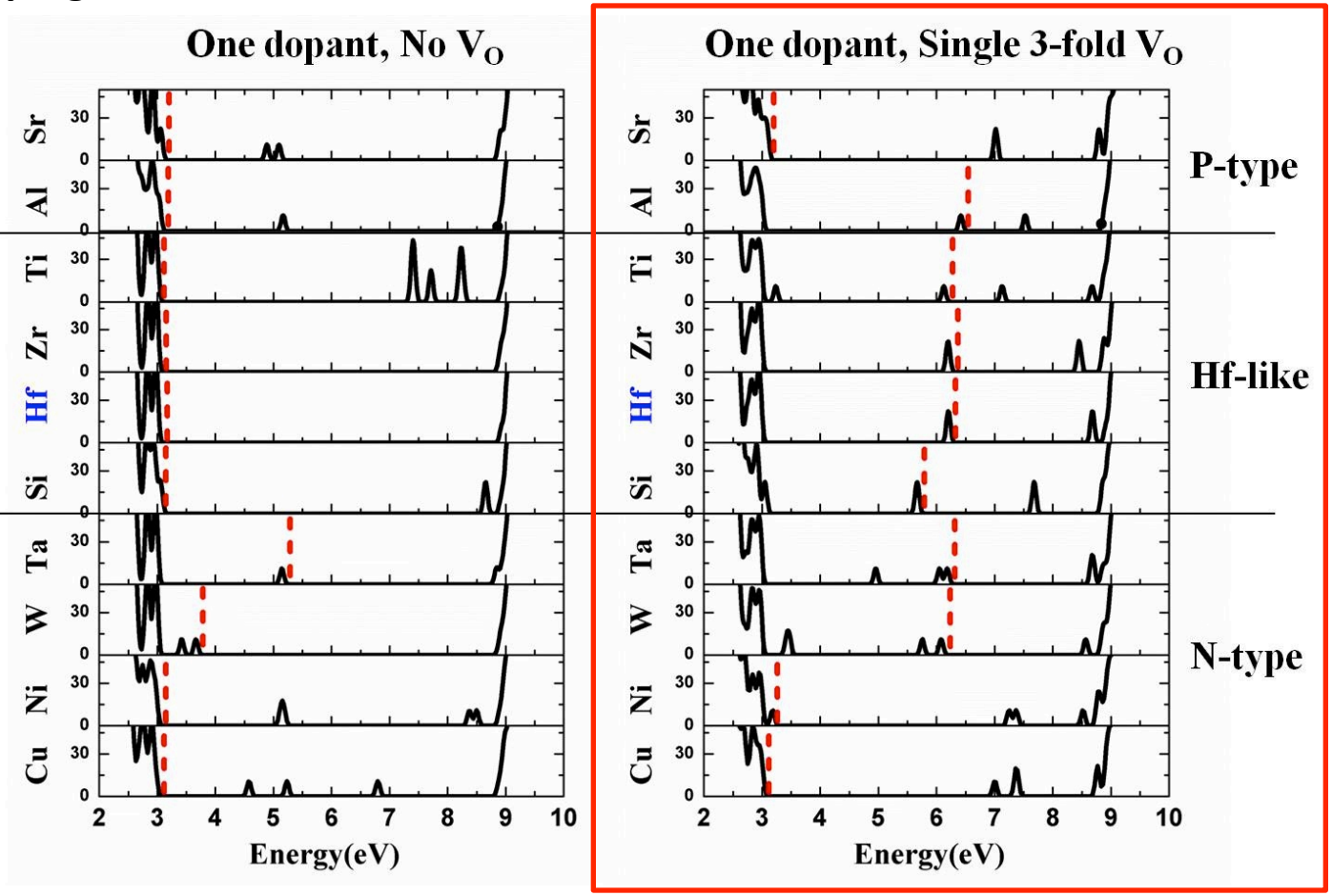

of valence d electrons
2
3
4
4
4
4
5
6
10
11

L. Zhao, S. Ryu, A. Hazeghi, D. Duncan, B. Magyari-Köpe, and Y. Nishi, VLSI 2013.

HfO_2: Vacancy Formation Energy Dopant + Filament

L. Zhao, S. Ryu, A. Hazeghi, D. Duncan, B. Magyari-Köpe, and Y. Nishi, VLSI 2013.

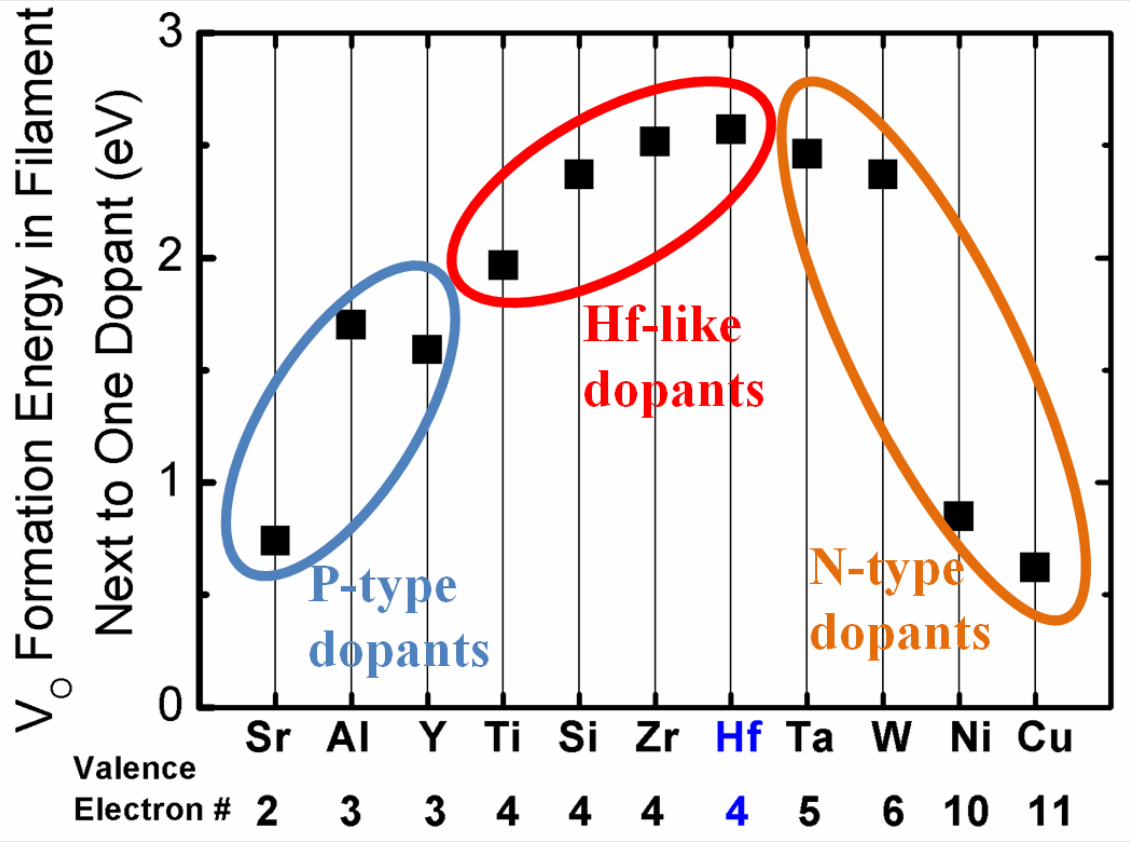

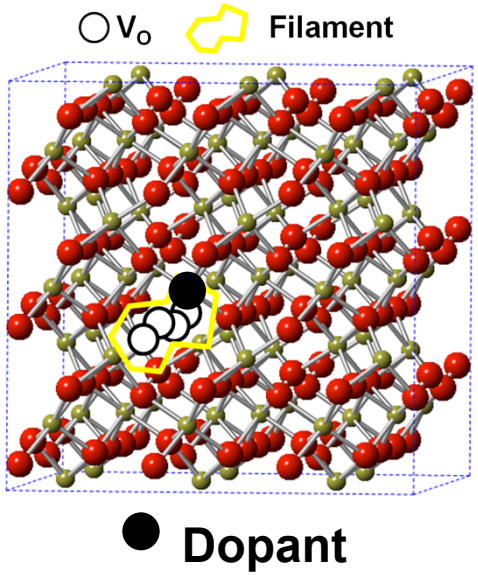

HfO_2: Partial Charge Density Dopant + Filament

Isosurface: 0.1 e/Å^3.

L. Zhao, S. Ryu, A. Hazeghi, D. Duncan, B. Magyari-Köpe, and Y. Nishi, VLSI 2013.

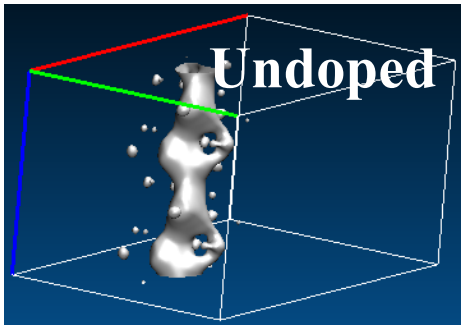

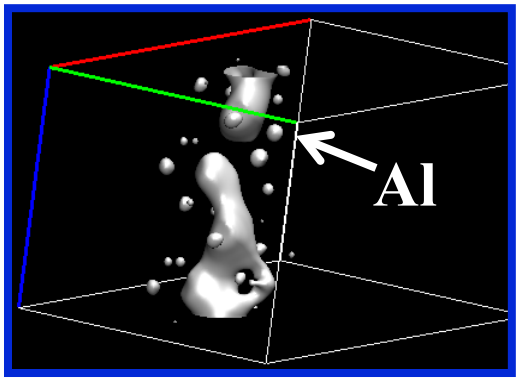

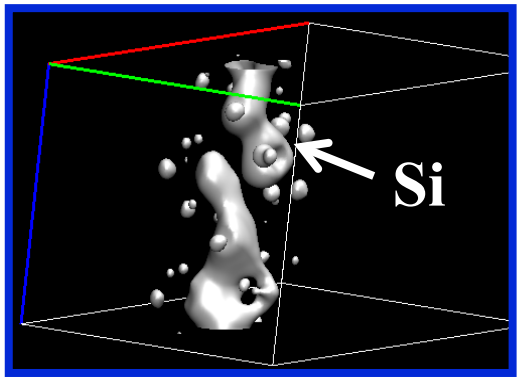

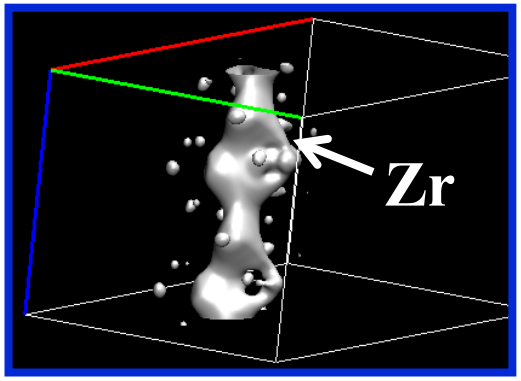

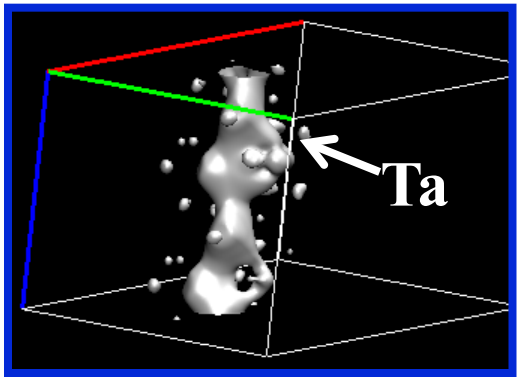

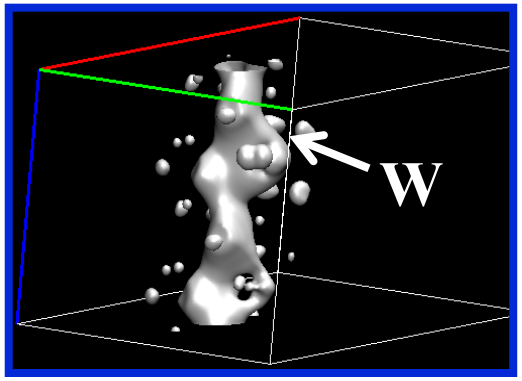

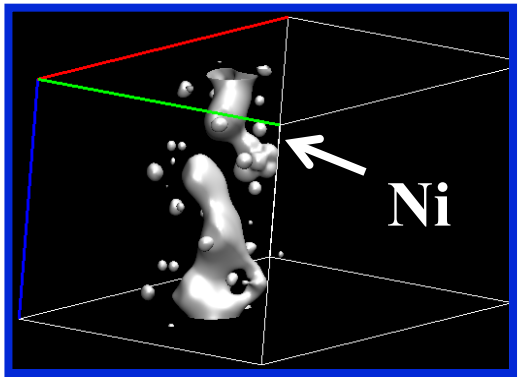

HfO_2 Doping: Experiments and Theory

L. Zhao, S. Ryu, A. Hazeghi, D. Duncan, B. Magyari-Köpe, and Y. Nishi, VLSI 2013.

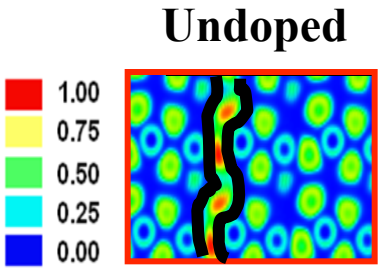

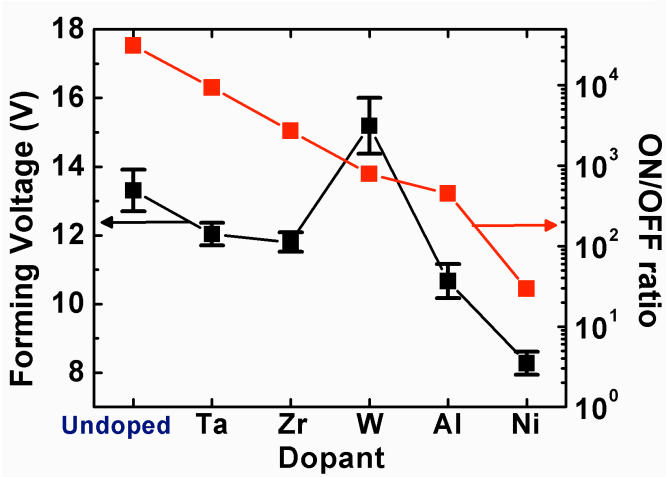

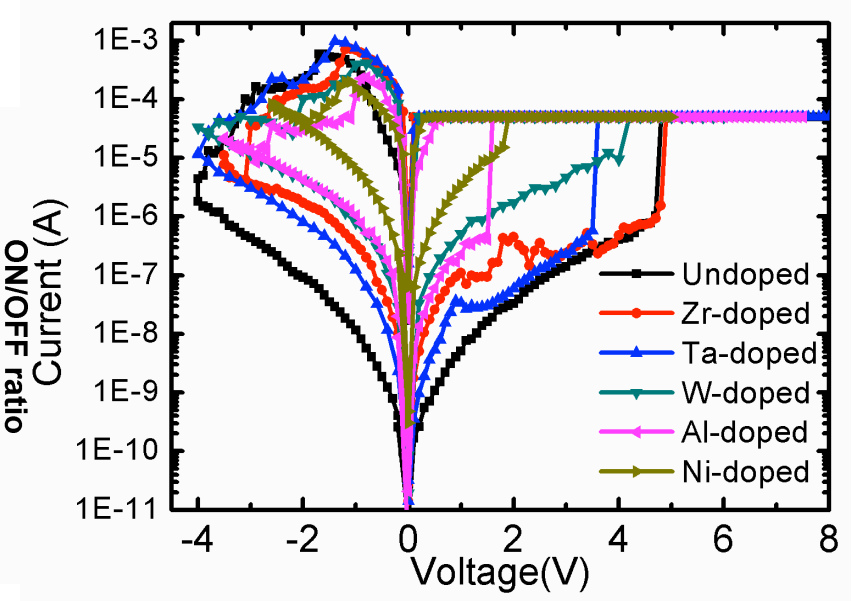

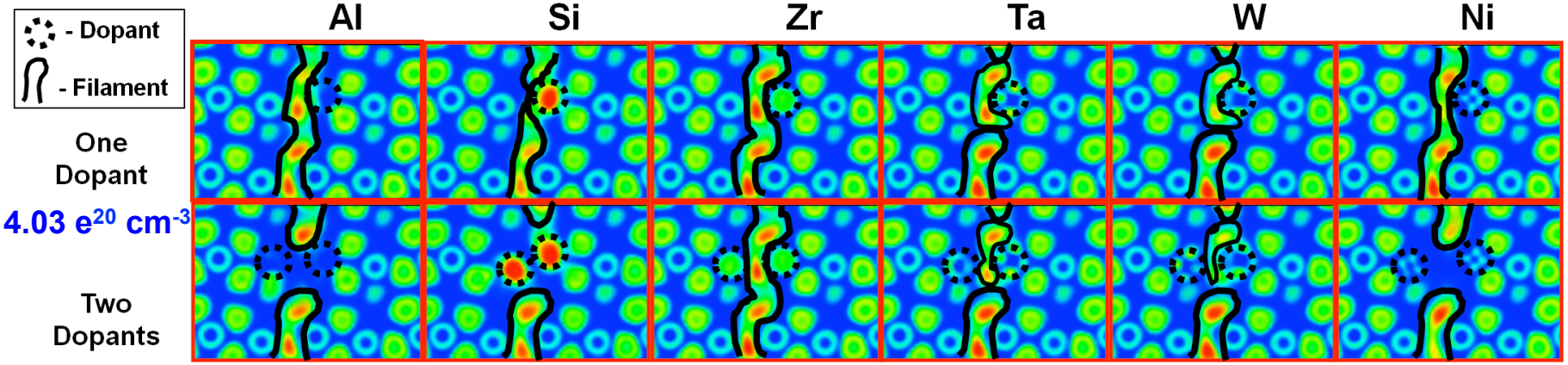

Outline

ON-state Conduction and Filament Formation: TiO_2, NiO, HfO_2, Al_2O_3

The Role of Dopants in Switching: TiO_2, HfO_2

Charge Trapping: TiO_2, HfO_2, Al_2O_3

Thermodynamics: Oxygen Diffusion in/out of the Filament: TiO_2

Electrode/Oxide Interfaces and Electronic Transport

Multilayer structures

Summary

Vacancy Diffusion Effect – Filament Rupture

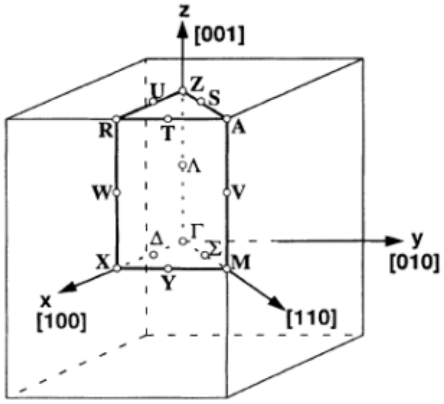

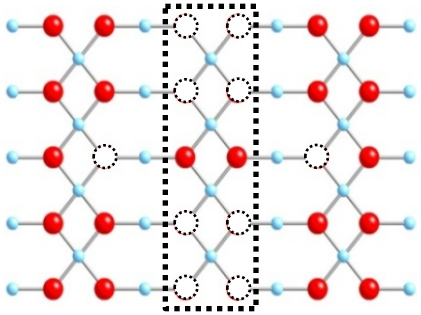

$2V_o$ off

Partial charge density

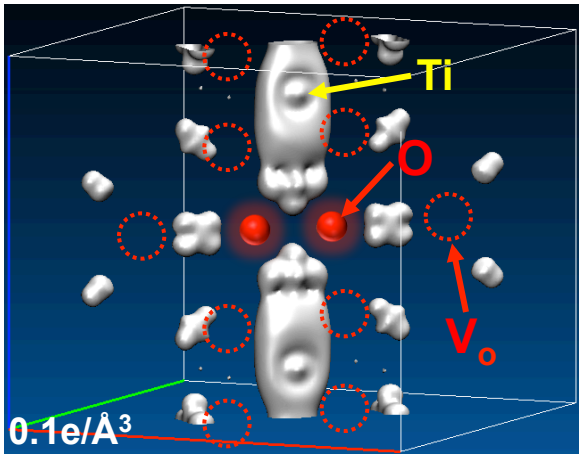

Spin up

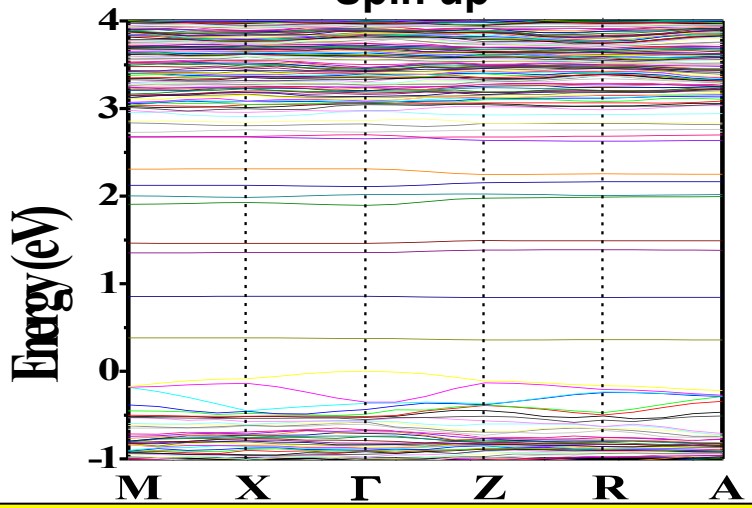

Spin down

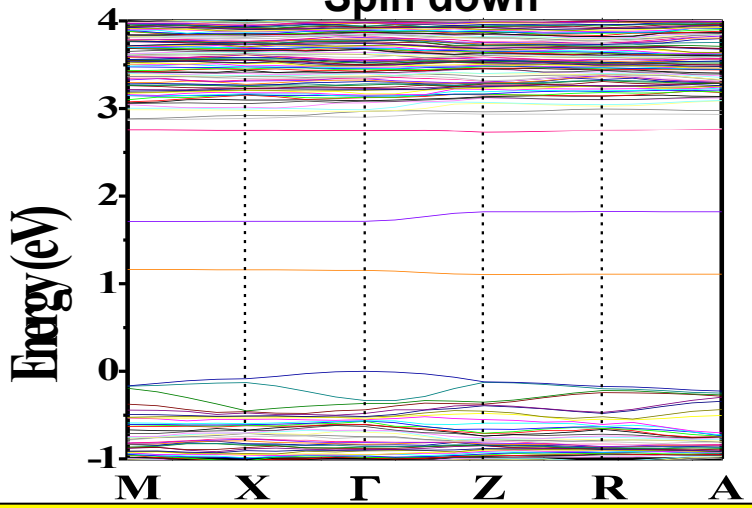

- **Strongly localized energy levels**
- **Significantly decreased electron conduction → increased resistivity.**

Charged Defect Formation Energies

TiO_2

"ON" - LRS state

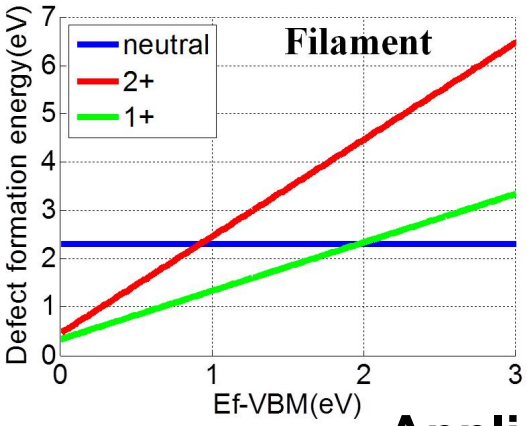

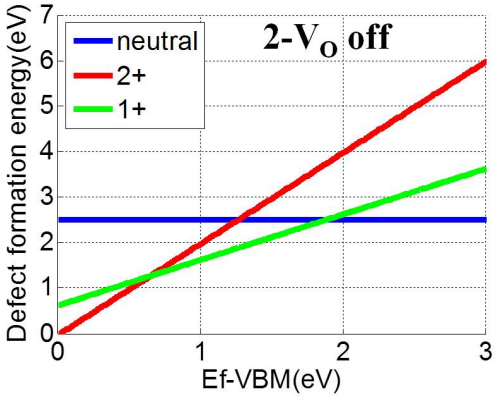

"OFF" – HRS state

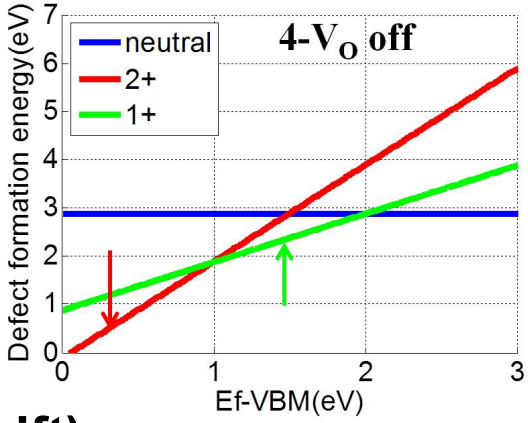

Applied voltage (Fermi Level Shift)

Injection of electrons - induces ordering of vacancies ->
stabilizes the filament.

Electron depletion – favors the formation of isolated vacancies ->
destabilizes the filament.

B. Magyari-Köpe et al., J. Mater. Sci., 47, 7498, 2012.

Charge Trapping – Filament Instability

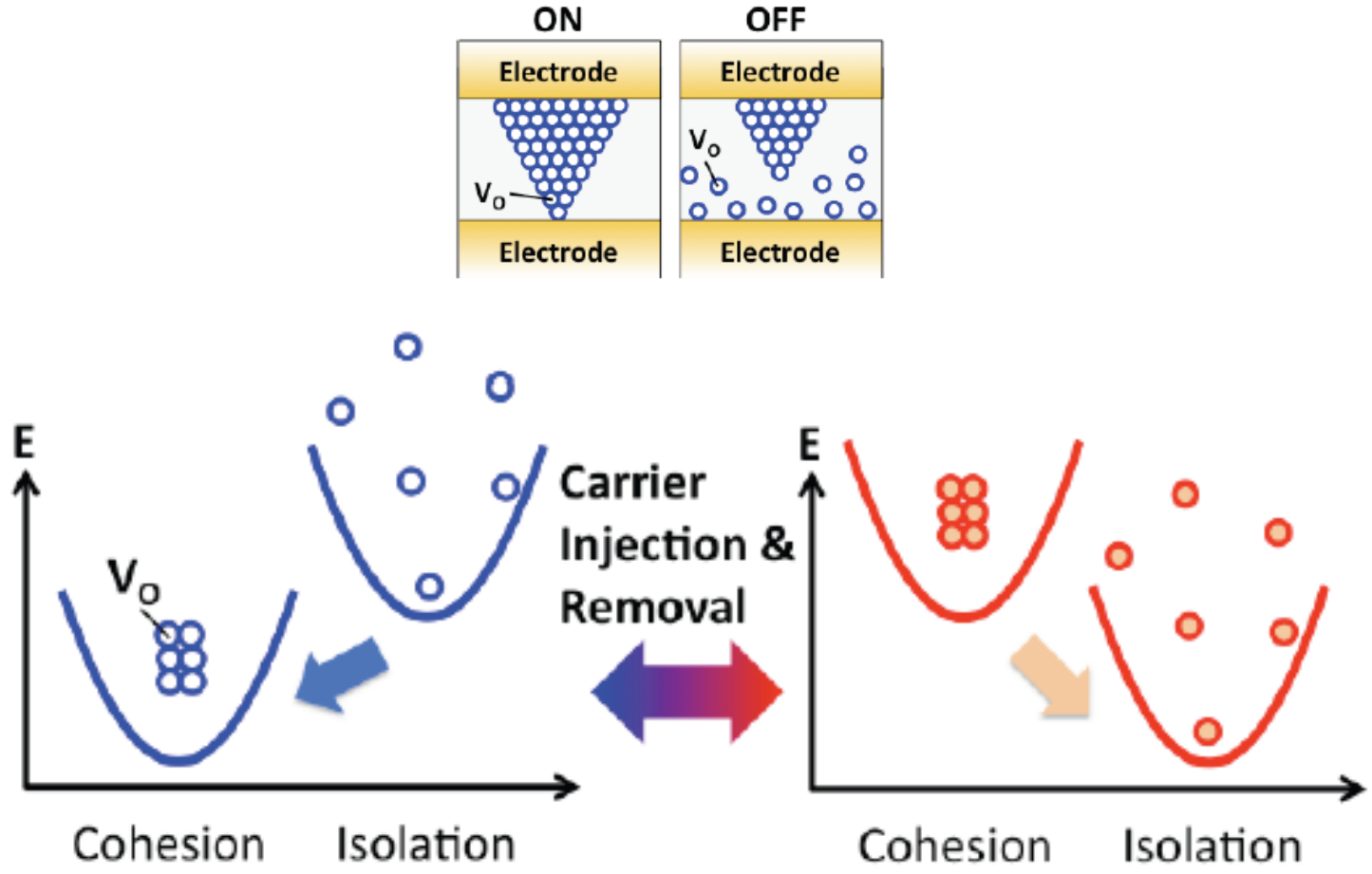

K.Kamiya, M.Y. Yang, S.G. Park, B. Magyari-Köpe, Y. Nishi, M. Niwa, and K. Shiraishi, APL 2012

V_0 Cohesion-Isolation Transition

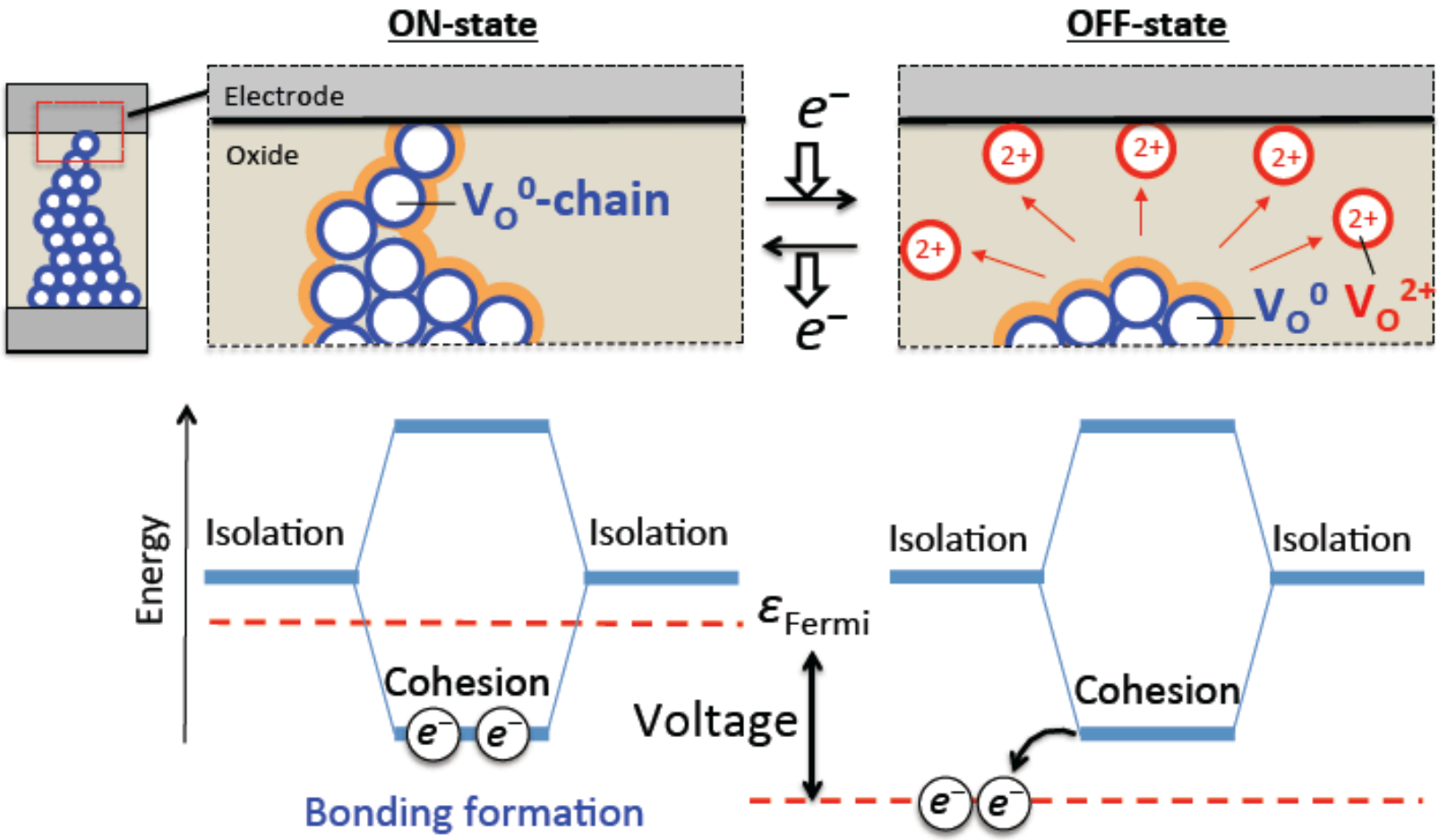

Cohesion/Rupture of Conductive Filaments in TiO_2, HfO_2, and Al_2O_3

$$E_C(q) = \frac{1}{n}\left[\{E(V_O^q - \text{chain}) + (n-1) \times E(\text{bulk})\} - n \times E(V_O^q - \text{isolated})\right]$$

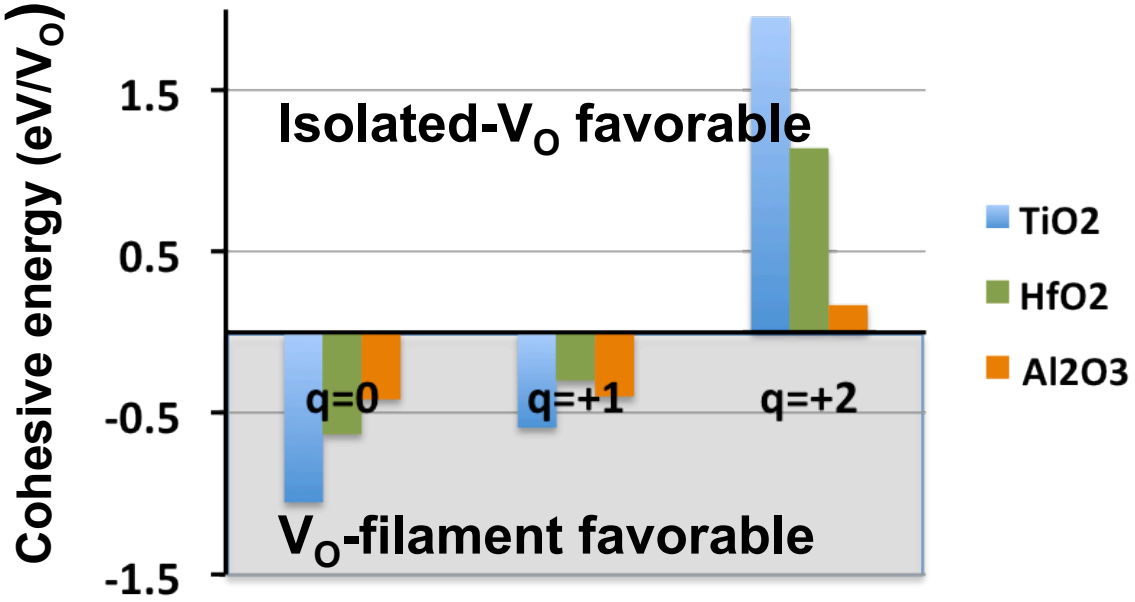

All three materials prefer to form V_O-filament in q=0 and q=+1 charge states.

K.Kamiya, M.Y. Yang, S.G. Park, B. Magyari-Köpe, Y. Nishi, M. Niwa, and K. Shiraishi, APL 2012

M.Y. Yang, K.Kamiya , B. Magyari-Köpe, Y. Nishi, H. Momida, T. Ohno, M. Niwa, and K. Shiraishi, SSDM 2012, JJAP 2013

Outline

ON-state Conduction and Filament Formation: TiO_2, NiO, HfO_2, Al_2O_3

The Role of Dopants in Switching: TiO_2, HfO_2

Charge Trapping: TiO_2, HfO_2, Al_2O_3

Thermodynamics: Oxygen Diffusion in/out of the Filament: TiO_2

Electrode/Oxide Interfaces and Electronic Transport

Multilayer structures

Summary

Thermodynamics of Oxygen Ion Diffusion into the Filament

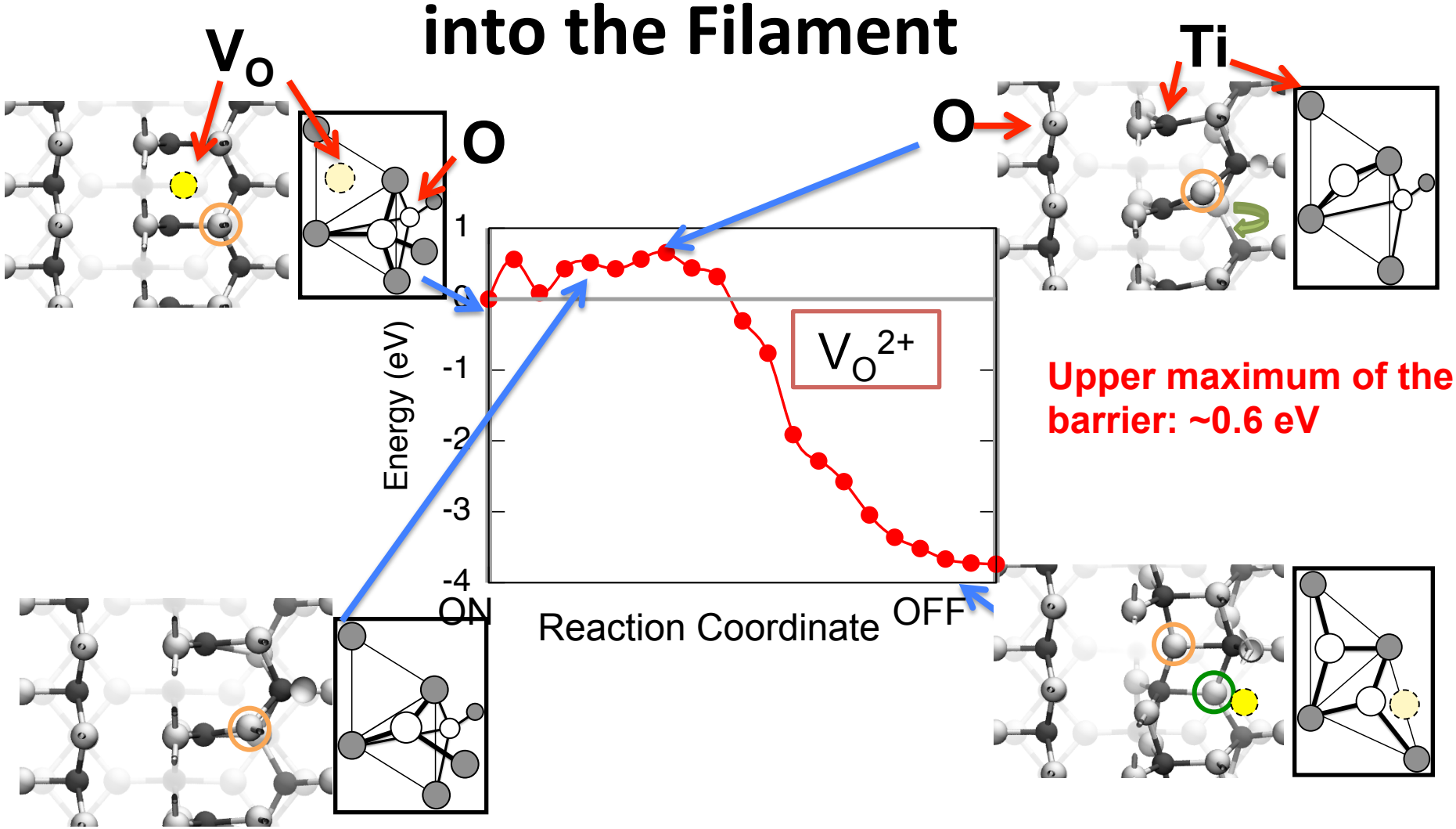

K. Kamiya, M. Y. Yang, B. Magyari-Köpe, M. Niwa, Y. Nishi, and K. Shiraishi, IEDM 2012.

Oxygen Vacancy Diffusion Barrier in/out of the Filament

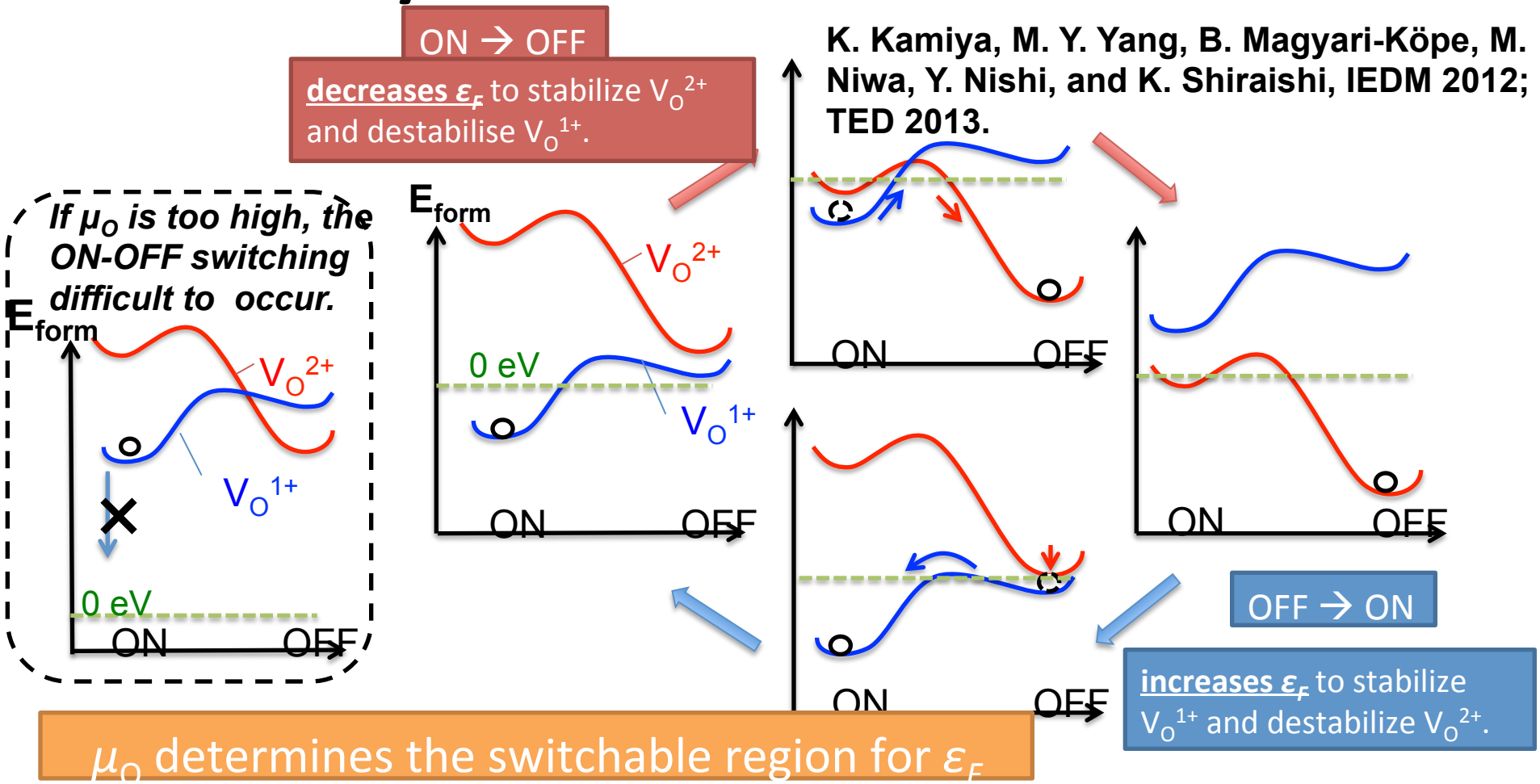

The O diffusion during the ON-OFF switching process is further enhanced by the applied electric field.

Outline

ON-state Conduction and Filament Formation: TiO_2, NiO, HfO_2, Al_2O_3

The Role of Dopants in Switching: TiO_2, HfO_2

Charge Trapping: TiO_2, HfO_2, Al_2O_3

Thermodynamics: Oxygen Diffusion in/out of the Filament: TiO_2

Electrode/Oxide Interfaces and Electronic Transport

Multilayer structures

Summary

Electronic Transport TiN/TiO_2/TiN (II)

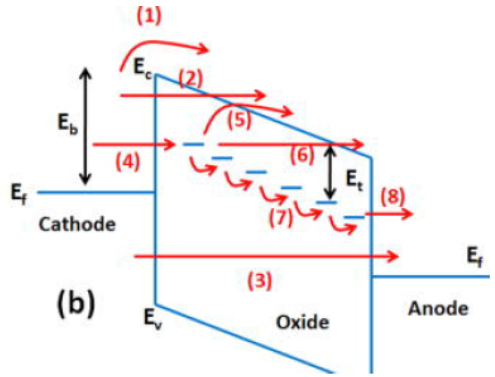

Electron transmission at finite biases: DFT-NEGF (ATK, QuantumWise, energy tolerance = 1e-6 eV, 8x8x1 k-points

Trap-assisted tunneling effects: modeled by isolated vacancies with various hopping distances (derived from nVo)

3VO, 3 nm

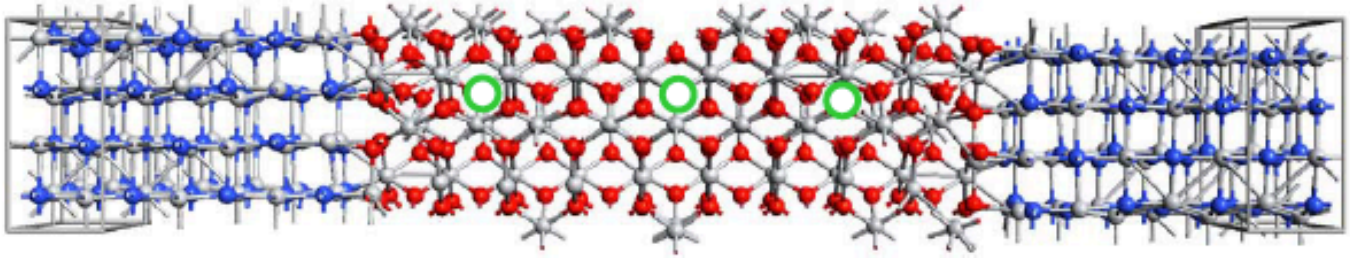

d_{hop}=0.8nm

1VO, 3 nm

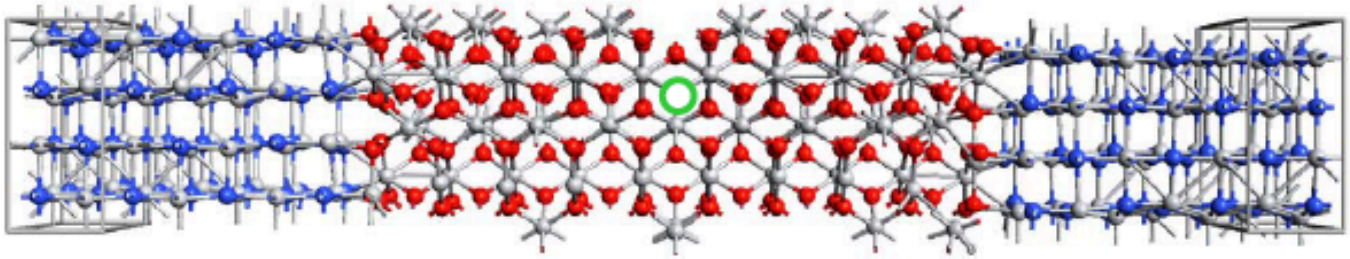

d_{hop}=1.4nm

Electronic Transport TiN/TiO_2/TiN (II)

NEGF calculations (QuantumWise ATK)

3.0nm oxide: perfect TiO_2 and isolated vacancies exhibit non-linear I-V, while both single and double vacancy filaments are metallic.

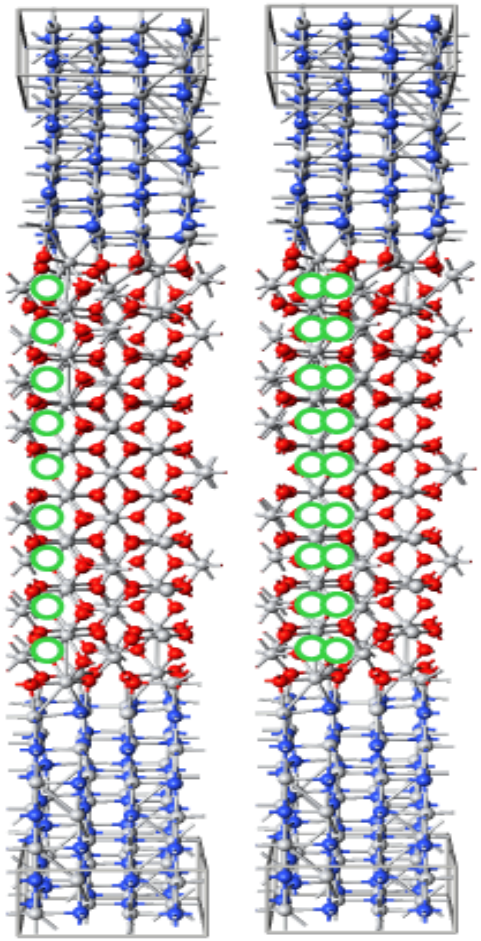

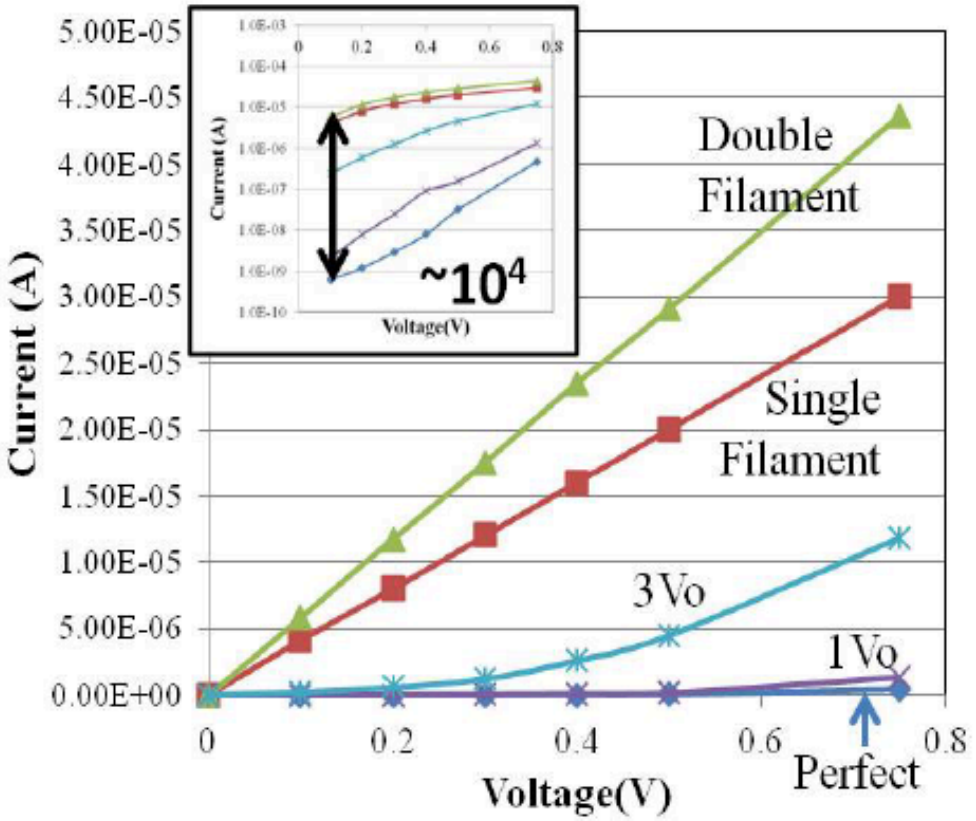

Zhao et al., APS 2013

Outline

ON-state Conduction and Filament Formation: TiO_2, NiO, HfO_2, Al_2O_3

The Role of Dopants in Switching: TiO_2, HfO_2

Charge Trapping: TiO_2, HfO_2, Al_2O_3

Thermodynamics: Oxygen Diffusion in/out of the Filament: TiO_2

Electrode/Oxide Interfaces and Electronic Transport

Multilayer structures

Summary

ReRAM stack structure with Al_2O_3 layer

Inserting Al_2O_3 layer

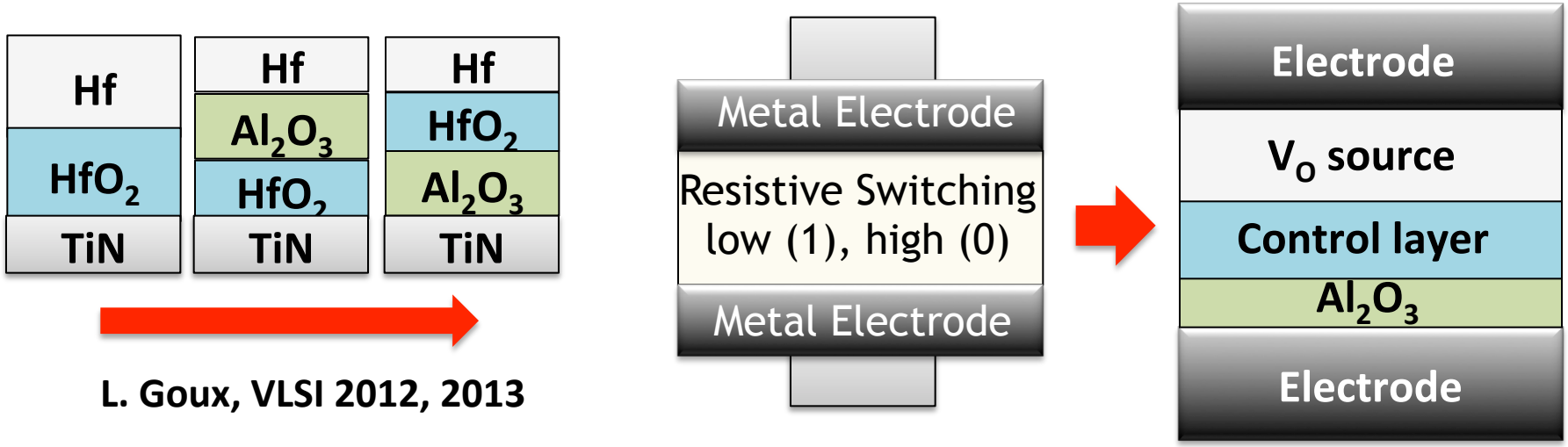

L. Goux, VLSI 2012, 2013

- From one- or two-layer stack structure to three-layer involving Al_2O_3 thin layer
- Increased ON/OFF ratio
- Goal: Lower the operation current and improve thermal stability for the stable switching operation.

Al_2O_3: Formation of O Vacancy Filament

Cohesive energy

$$E_C(q) = \frac{1}{n}\left[\{E(V_O^q - \text{chain}) + (n-1)\times E(\text{bulk})\} - n \times E(V_O^q - \text{isolated})\right] \quad (n = 8)$$

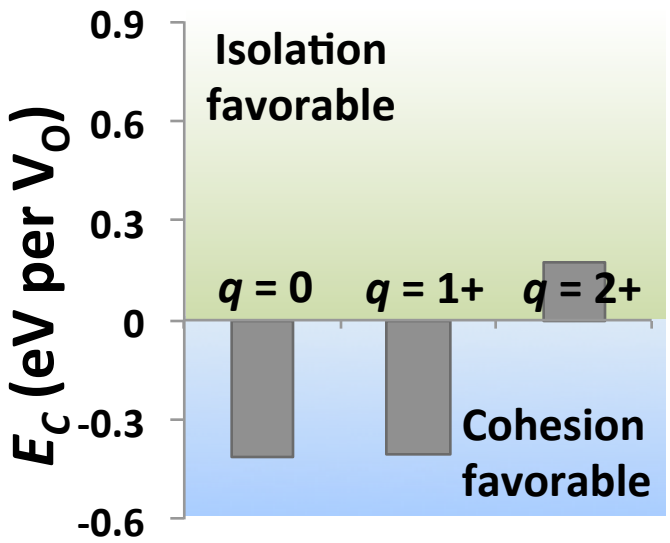

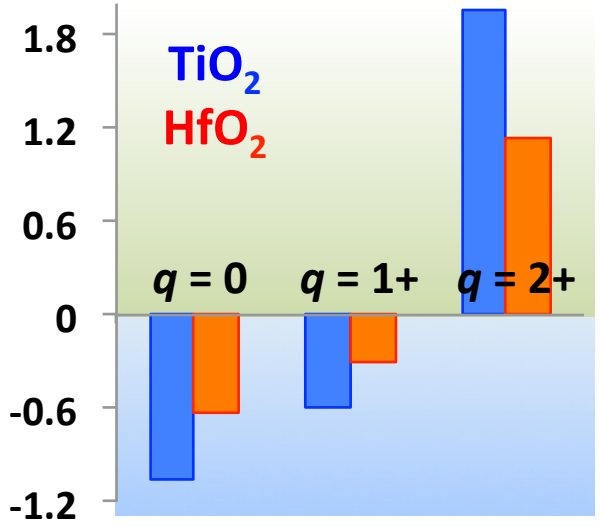

K. Kamiya, APL 2012; IEDM 2012, PRB 2013, TED 2013

- An isolated V_O tends to become cohesive when q = 0 and 1+.
- The cohesive energy is about 0.4 eV for q=0/1+ charge states

ON/OFF switching in a multilayer structure

Three-layer structure

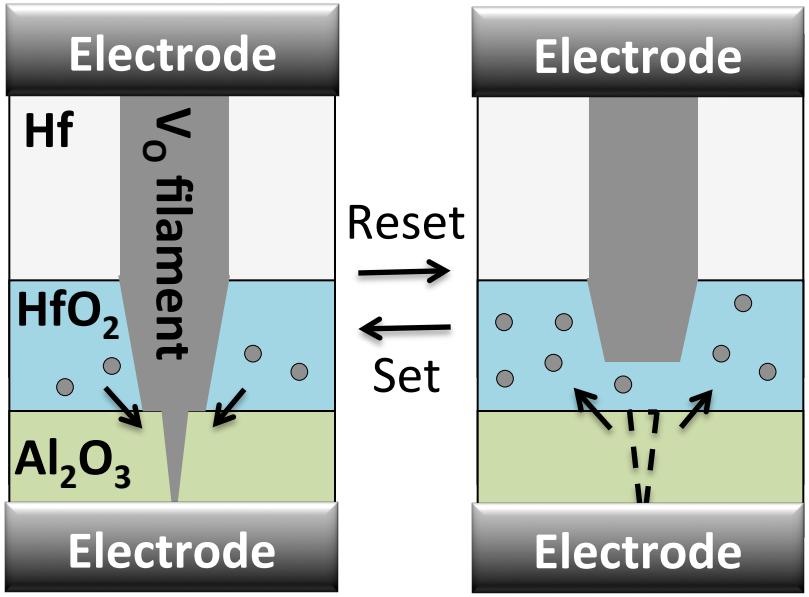

One- or Two-layer structures

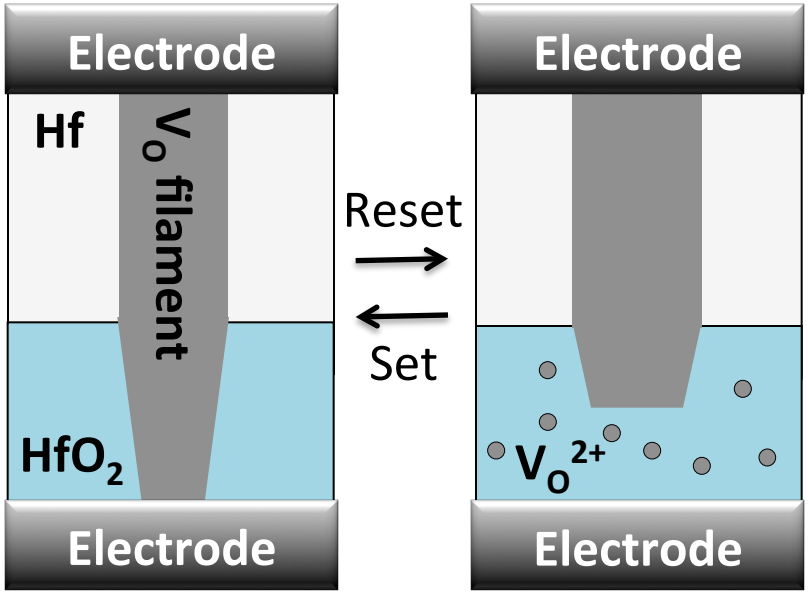

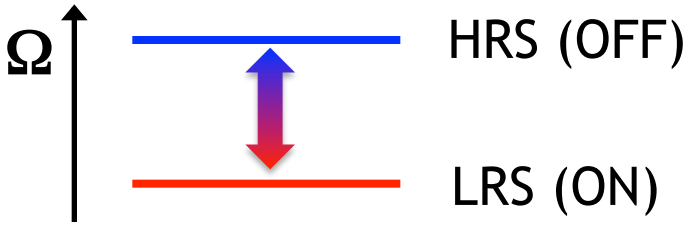

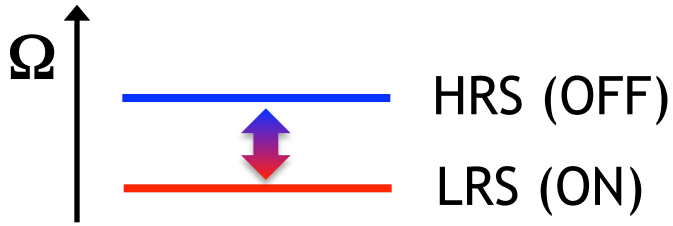

- Al_2O_3 - O interstitial former.
- The physical mechanism of Al_2O_3 inducing high ON/OFF ratio?

Model of O Vacancy Filament growth (I)

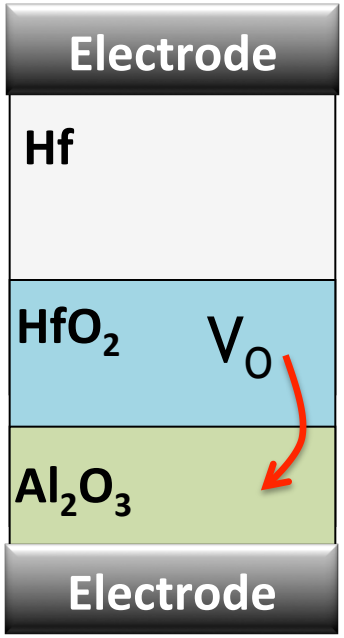

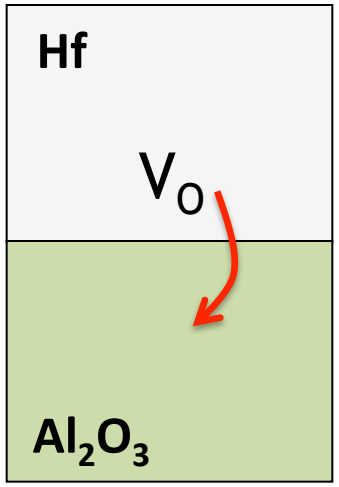

K. Kamiya et al., IEDM 2012; TED 2013
M Yang et al., SSDM 2012, JJAP 2013

$$Al_2O_3 + ½(Hf) \longrightarrow Al_2O_3\ (V_O) + ½(HfO_2)$$

V_O formation energy in Al_2O_3: 8 eV

$$E_f = \{E(V_O) - E(\text{bulk})\} + \mu_O$$

Heat of formation of HfO_2 : —5.8 eV (per one O atom)

$$Hf + O_2 \rightarrow HfO_2$$

- **Formation of V_O costs 2.2 eV energy loss even when Al_2O_3 is in contact with Hf (Hf-rich V_O source).**

Band Offsets $TiN/Al_2O_3/Hf$

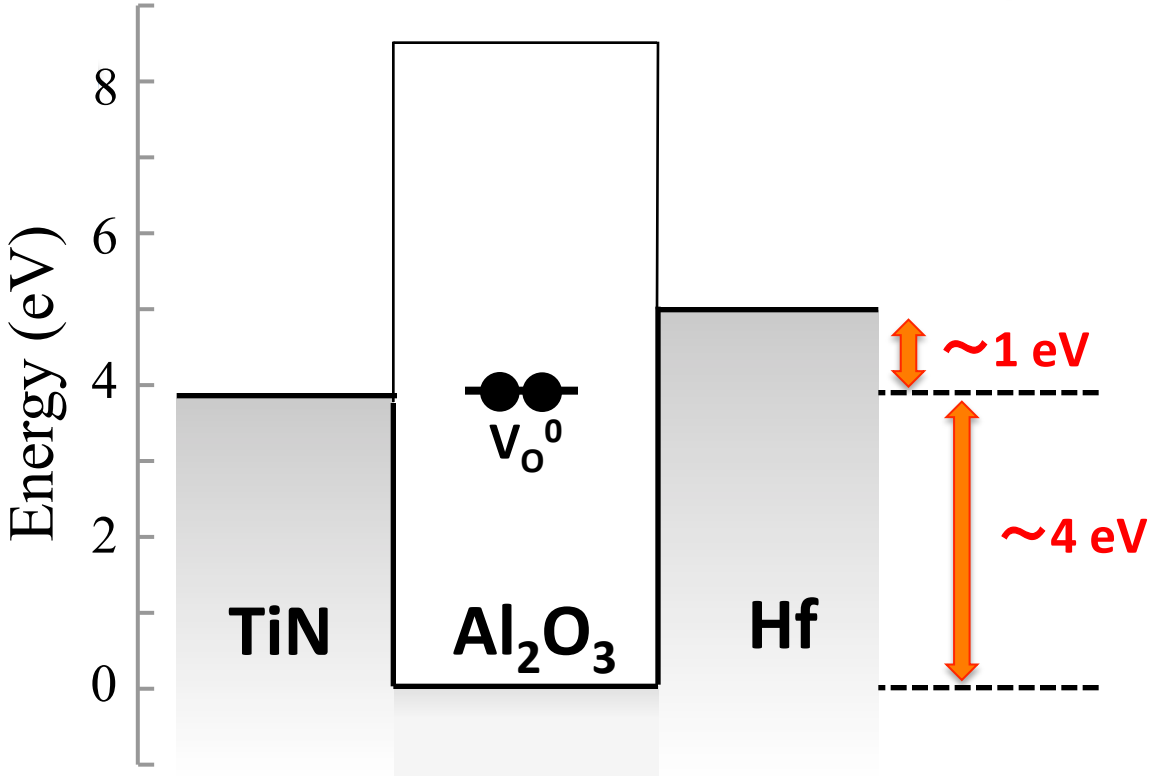

- Fermi level of TiN is almost the same as the V_O level of Al_2O_3 and about 4 eV higher than VB of Al_2O_3.
- Fermi level of Hf is roughly 1 eV higher than that of TiN.

Model of O Vacancy Filament growth (II)

K. Kamiya et al., IEDM 2012; TED 2013
M Yang et al., SSDM 2012, JJAP 2013

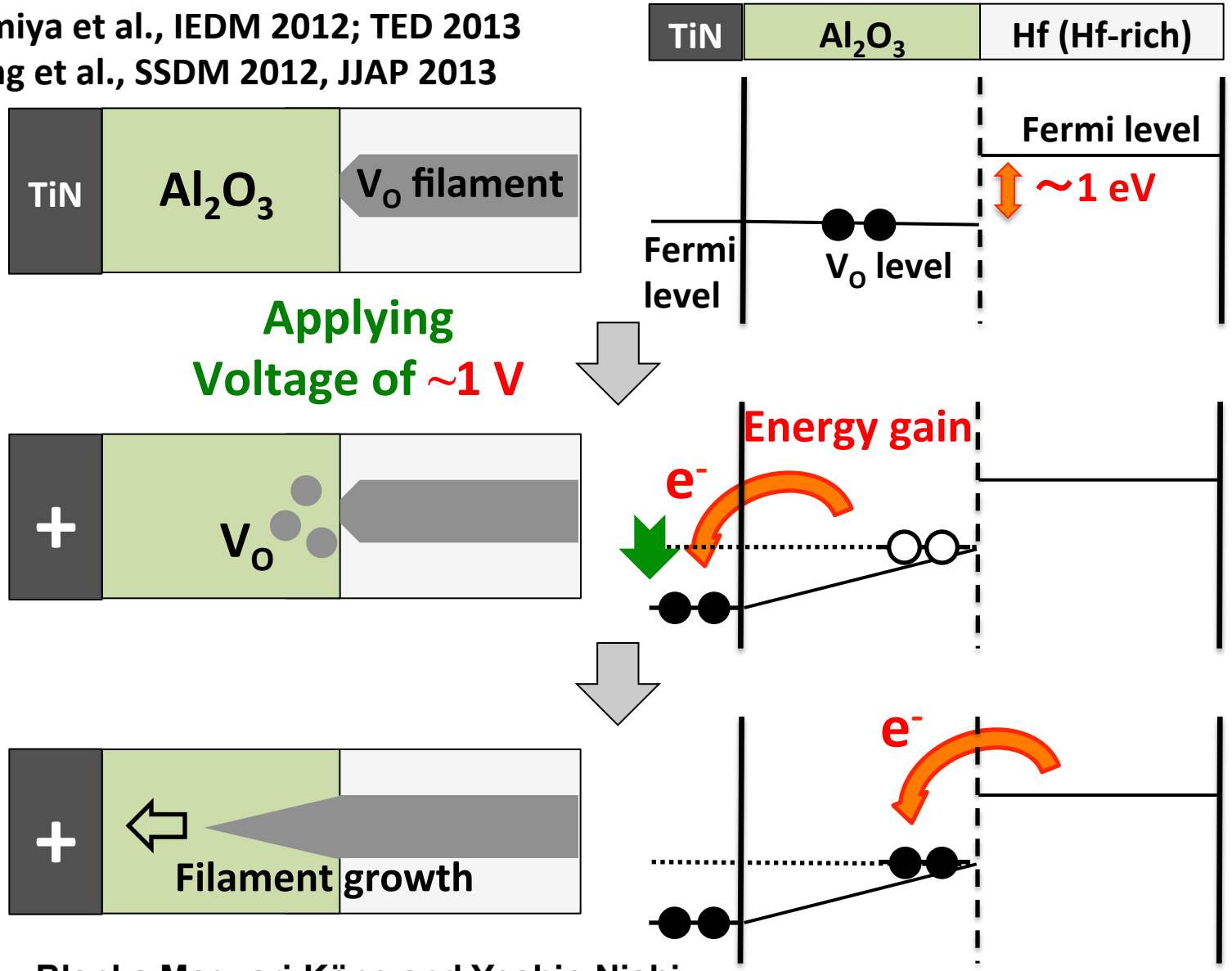

Model of O Vacancy Filament growth (III)

K. Kamiya et al., IEDM 2012; TED 2013
M Yang et al., SSDM 2012, JJAP 2013

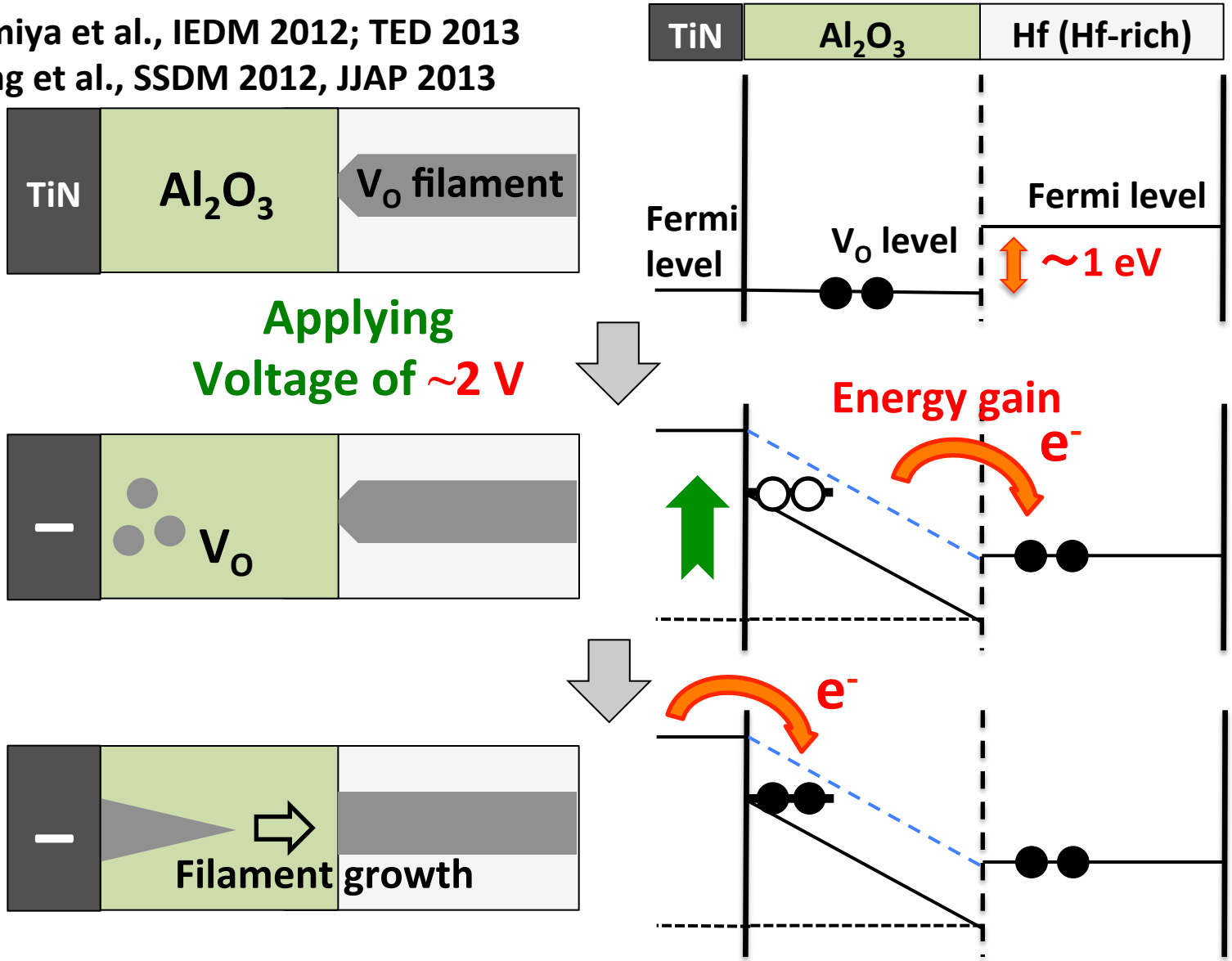

Summary

- A filamentary arrangement of oxygen vacancies may account for the higher conductivity observed in oxygen deficient TiO_2, NiO, HfO_2 and Al_2O_3.
- The filament rupture process during the ON-OFF switching can be further enhanced/blocked by dopants diffusion into the vacancy sites – and the process is strongly enhanced by the applied electric field.
- Vacancies at the electrode/oxide interfaces influence the conductivity and ionic transport. Based on NEGF calculations: the electron transport change from a metallic type through the filaments to an isolated trap assisted model bears a 10^4 change in the ON/OFF ratio.
- Multilayer structures – control of the oxygen chemical potential and electric field is required